BUREAU OF RECLAMATION

Intuitive Quantitative Metrics for Rapid Assessment of Entrainment Risks and Salmonid Responses in The Delta

California Great Basin Region

Bay-Delta Office

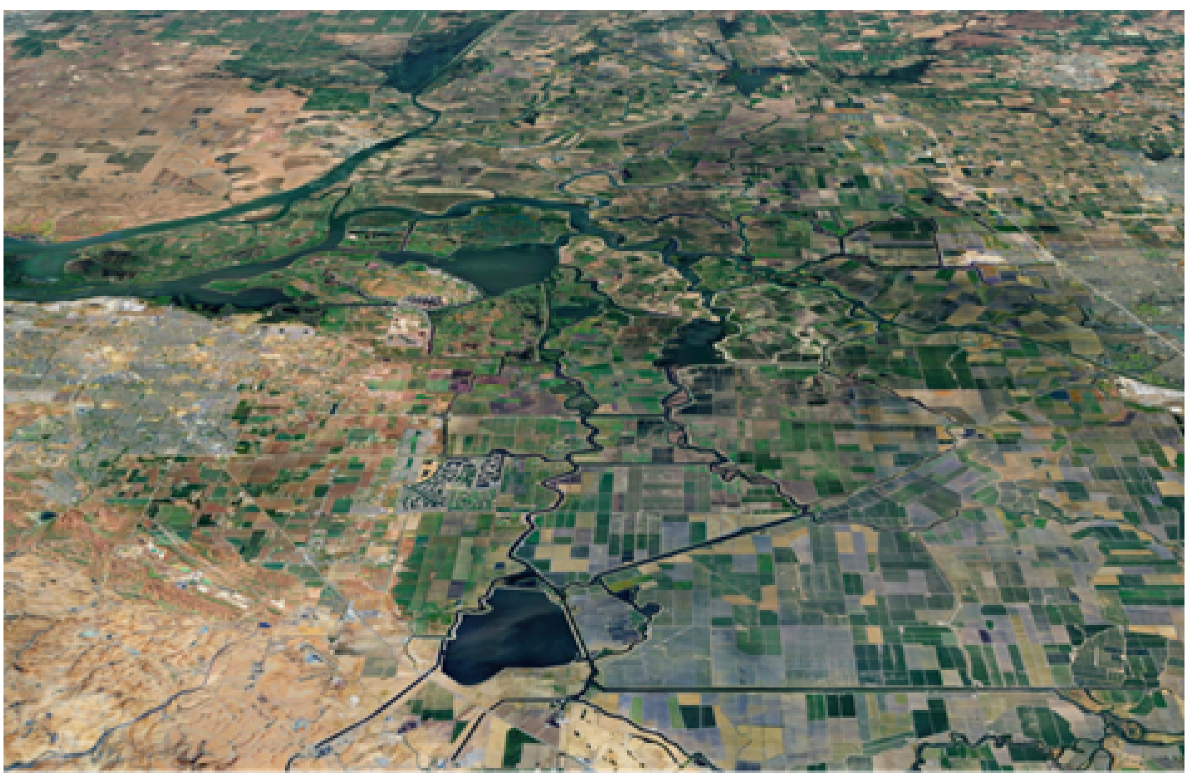

Cover Photo: Aerial photo of the Sacramento-San Joaquin Delta from Google Earth, accessed May 12, 2026.

U.S. Department of the Interior

May 2026

Mission Statements

The U.S. Department of the Interior protects and manages the Nation's natural resources and cultural heritage; provides scientific and other information about those resources; honors its trust responsibilities or special commitments to American Indians, Alaska Natives, and affiliated Island Communities.

The mission of the Bureau of Reclamation is to manage, develop, and protect water and related resources in an environmentally and economically sound manner in the interest of the American public.

Intuitive Quantitative Metrics for Rapid Assessment of Entrainment Risks and Salmonid Responses in The Delta

California Great Basin Region

Bay-Delta Office

Prepared by:

Ching-Fu Chang, PhD
Contra Costa Water District
1331 Concord Ave
Concord, CA 94520

Contents

Tables

Figures

Acronyms

cfs	cubic feet per second
CSAMP	Collaborative Science and Adaptive Management Program
CVP	Central Valley Project
CWT	Coded Wire Tag
DCC	Delta Cross Channel Gates
Delta	Sacramento-San Joaquin River Delta
DSP	Delta Science Program
DWR	California Department of Water Resources

ESA	Federal Endangered Species Acts
LTO	Long-term Operation
NAS	National Academies of Sciences, Engineering, and Medicine
OMR	Old and Middle River
OMRI	Old and Middle River Index
PEL	Proportional Entrainment Loss
PTM	Particle Tracking Module
RMSE	root mean squared error
SWP	State Water Project

1. Introduction

Operation of the Central Valley Project (CVP) and State Water Project (SWP) affect the movement and survival of threatened and endangered species in the Sacramento–San Joaquin Delta (Delta), California. The U.S. Department of Interior, Bureau of Reclamation (Reclamation) and the California Department of Water Resources (DWR) adjust operations with actions, such as closing the Delta Cross Channel gates, operating behavioral barriers at Georgiana Slough, or limiting export pumping, to reduce the routing of fish into the central and south Delta and entrainment into the Tracy Fish Collection Facility and Skinner Delta Fish Protective Facility (collectively, salvage facilities). Balancing water supply and protections for species requires the ability to evaluate the effects of alternative operations on species responses such as routing, entrainment, and through-Delta survival.

For some time, including in the most recent Endangered Species Act (ESA) and California Endangered Species Act consultations (California Department of Fish and Wildlife 2024; National Marine Fisheries Service 2024; U.S. Fish and Wildlife Service 2024), net Old and Middle River (OMR) flow has been used as an indicator of overall transport and entrainment risk for smelts and salmonids. However, OMR does not capture the significant differences in hydrology throughout the Delta or the tidal advective-dispersive transport in the Delta, and entrainment risk can differ under the same OMR level. Furthermore, real-time adjustments of the OMR level may be determined in closed discussions, or in some cases ill-supported by hydrodynamics, which in turn leads to uncertainty for the communities that depend on the water supplies and the regulatory agencies charged with evaluating potential effects to species. On the other hand, physics-based hydrodynamic models of the Delta capture the underlying mechanisms more completely, but their setup and execution require substantial technical preparation that limits their use in routine operational decisions

This study bridges the gap between simple proxies and arduous modeling. Specifically, our research objective is to develop tools that (1) account for the tidal advective-dispersive transport and the spatial heterogeneity of entrainment risk in the Delta, (2) have considerably lower requirements for input data and computational resources than Delta hydrodynamic models do, and (3) are intuitive and implementable in the context of real-time operations management and regulation. To that end we developed two sets of tools that allow users to estimate the outcomes of more rigorous modeling and get straight to the hydrodynamic insights:

- Hydrodynamic model emulators, which are machine learning models that estimate the key hydrodynamic model outputs most relevant in the context of operations management (e.g., particle entrainment at CVP and SWP export facilities).
- Hydraulic footprints, which are spatially informed summary metrics for transport and entrainment risk in the central and south Delta.

2. Background

Delta Hydrodynamics

The Sacramento-San Joaquin Delta receives inflows from the Sacramento River (about 80% of Delta inflow, on average), the San Joaquin River (about 15% of Delta inflow, on average), and other eastside tributaries and precipitation. The mass balance is completed by Delta outflow (about 75% of Delta inflow, on average), CVP and SWP exports (Jones Pumping Plant pumping and Clifton Court Forebay inflow, respectively, collectively about 20% of Delta inflow on average), and other in-Delta uses and diversions.

However, while long-term averages hold, the Delta is more complex than individual flow metrics. Effects of intra- and inter-annual variability are significant in both the hydrologic conditions and the operations of CVP and SWP. For example, Delta inflows can vary between years by an order of magnitude; closure of the Delta Cross Channel Gates (DCC) and the operation of a non-physical barrier on Georgiana Slough can reroute flows or fish; and localized storms over the San Joaquin Basin can double the contribution of flows from that basin and dominate hydrodynamics in the south Delta. The DAYFLOW database provides long-term daily measured or estimated flow data, including the net Delta outflow index and various component flows (California Department of Water Resources n.d.), and is a valuable dataset to demonstrate the variability behind long-term averages. On top of that, tidal cycles reverse flows twice a day in the Delta channel network, resulting in variability an order of magnitude greater than daily averages at sub-daily time scales (e.g., plus or minus 20,000 cubic feet per second, or cubic feet per second (cfs), in Old River or Middle River, and plus or minus 100,000 cfs at the Sacramento-San Joaquin Rivers confluence). The hydrologic conditions, operations, and the tidal effects together shape the hydrodynamic scenarios in the Delta.

Hydrodynamics drive transport in the Delta, which, in combination with fish behavior, affects the risk of entraining protected species at the CVP and SWP export facilities. Physics-based hydrodynamic models of different levels of complexity have been applied in the Delta in various studies, including Delta Simulation Model II (Fleenor and Bombardelli 2013; Sridharan et al. 2018), UnTRIM Bay-Delta Model (Gross et al. 2019 and 2022; MacWilliams et al. 2015), and Bay-Delta SCHISM (Zhang et al. 2020). Among these, DSM2 is the most common model in applications, partly because it strikes a satisfactory balance between computational demand and model fidelity with its one-dimensional formulation. DSM2 consists of modules that can simulate hydrodynamic outputs (HYDRO) as well as the fate and transport of water quality constituents (QUAL and GTM) or particles (PTM and ECO-PTM). DSM2 HYDRO captures the tidal advective-dispersive dynamics that scalar flow metrics cannot represent. However, these hydrodynamic models require substantial technical preparation for each run, including boundary condition specification, model spin-up, and post-processing, that limits their use in resource-limited scenarios such as real-time analyses.

Entrainment Management

The Delta Smelt Monitoring Analysis and Synthesis Team Report (Interagency Ecological Program 2015) and the Salmon and Sturgeon Assessment of Indicators by Life stage report (Windell et al.

2017) provide conceptual models that identify stressors on species in the Delta. The CVP and SWP affect entrainment stressors through (1) the alteration of flows that influence route selection and survival of out-migrating salmonids and migrating adult, larval, and juvenile smelts; and (2) direct entrainment and loss of fish at the export facilities.

The net OMR, has been the primary operational metric governing CVP and SWP entrainment management for listed species since its formalization in the 2008 and 2009 Biological Opinions (National Marine Fisheries Service 2009; U.S. Fish and Wildlife Service 2008). OMR is a Eulerian flow metric representing the combined net advection at two specific locations along the Old and Middle River corridor and was developed in studies of Delta pelagic organism decline for its practical convenience as an indicator of transport and entrainment risk. More negative OMR represents more flow towards export facilities while more positive OMR represents less flow towards export facilities. Export management has evolved since the introduction of OMR, and real-time operations now consider a range of factors including index equations, storm-flow conditions, particle tracking model results, species status and distribution, and estimates from species-response models. Most operational requirements, however, remain defined in terms of OMR thresholds, and implemented through a calculated OMR Index (OMRI) approximation due to practical constraints on measuring OMR. OMRI is a spline multiple linear regression model (Hutton 2008). The use of OMRI in practice introduces additional uncertainties, as its value can sometimes deviate from OMR by hundreds to thousands of cfs during the OMR management season.

Delta Smelt Survival

The proportional entrainment framework developed by Kimmerer et al. (2008) related export rates to the fraction of the Delta Smelt population exposed to entrainment. Proportional Entrainment Loss (PEL) metrics derived from this framework have been used to assess the population-level significance of entrainment events relative to total population size. The Delta Smelt Scoping Team within the Collaborative Science and Adaptive Management Program (CSAMP) evaluated factors associated with salvage of adult smelt and found that swimming behaviors were more complex than explained by PTM simulations (Grimaldo et al. 2020). Tillotson and Brandon (2023) evaluated sub-adult survival and identified covariates of OMR and PEL and found high sensitivity to entrainment of this life stage. Smith et al. (2021) evaluated how entrainment mortality propagates through population dynamics across life stages, and this life cycle model has been applied in the environmental review process of the Long-Term Operation of CVP and SWP (hereinafter, LTO) to assess population-level effects of alternative export management scenarios.

Salmonid Survival and Routing

Early analyses using Coded Wire Tag (CWT) data from fall-run and winter-run Chinook salmon documented a negative relationship between export rates and downstream recovery, supporting the initial conceptual model underlying the OMR metric (Newman 2003; Newman & Rice 2002). Hierarchical Bayesian models applied to the same CWT datasets through the mid-2000s found varying evidence for export effects depending on origin, reach, and model structure, with some analyses finding equal statistical support for export-based, inflow-based, and null models (Newman 2008; Newman & Brandes 2010). Other contemporary models include:

- The Delta Passage Model assembled reach-specific survival and routing relationships into a simulation framework for the interior Delta, comprising 10 reaches and four junctions and drawing on both acoustic telemetry and CWT-based survival estimates calibrated to the range of observed conditions (Cavallo et al. 2011).

- The Survival and Routing (STARS) model (Perry et al. 2018) formalized acoustic telemetry-based estimation of survival and routing probabilities for juvenile Chinook salmon migrating through the Delta network from the Sacramento River. STARS analyses have documented that survival is strongly influenced by route selection at key junctions, particularly the Delta Cross Channel and Georgiana Slough, and that route selection itself is influenced by gate operations and flow conditions rather than by export rates directly.

- The DSM2 Ecological Particle Tracking Module (ECO-PTM) was developed to provide a mechanistic bridge between hydrodynamic conditions and through-Delta survival of salmonids. ECO-PTM was calibrated with the travel data of acoustic tagged hatchery Chinook salmon released in the Sacramento Basin, and also integrated local and regional survival and routing models from prior studies (Wang et al. 2024). ECO-PTM uses a random walk technique for swimming behaviors and tracks the travel time, route selection, and route-specific survival of individual particles with simulated salmonid behaviors. The model for San Joaquin-origin Chinook salmon is still under development.

The CSAMP Salmonid Scoping Team synthesized the scientific literature in 2017 across the full range of studies on the relationship between exports, inflows, and salmonid survival in the Delta (Buchanan & Ferguson 2017a, 2017b). The CSAMP Salmon Technical Working Group, convened in 2023–2024 to review updated science relevant to life cycle and decision support models, found no significant improvement in through-Delta survival associated with the range of OMR flows under the conditions studied (Ferguson & Cavallo 2024). This supports a hypothesis that the influence of exports on route selection and survival of salmonids is limited under the current range of management; however, it does not define whether increased exports may cross a threshold and exert larger effects.

Detections in Salvage and Loss

Fish entrained into the central and south Delta experience lower survival and may either swim out of the interior Delta volitionally or, if they reach the salvage facilities, be trucked to release locations in the western Delta. Salvage, namely the process of capturing entrained fish at the CVP and SWP facilities and releasing them back to the Delta, can be effective for salmonids, but does not perform well for larval and juvenile smelts, which have weaker swimming capabilities and thus behave more similarly to passive particles. Salvage is a valuable species response and the subject of many studies on entrainment, because it connects observed data (from salvaging) to the unknown true state of species entrainment. Models for salvage of salmonids include:

- The Salvage Density Model, which estimates daily entrainment loss as a function of export rates applied to observed salvage data (Reclamation 2025a).

- A quantile regression random forecast model to estimate entrainment risk over a one-week forecast horizon using the previous week's entrainment loss, Sacramento River flow, and export rates as primary predictors (Tillotson et al. 2022).

- The Winter-Run CWT Proportional Salvage Model, which applies a zero-inflated negative binomial regression to estimate the fraction of the winter-run Chinook salmon population at risk of salvage under forecast hydrologic conditions (Zeug & Cavallo 2014).
- Delta Export Zone of Influence Analysis, using simulated velocities from DSM2 HYDRO and Gaussian kernel density estimation to map the spatial extent of hydraulic alteration attributable to different export levels, providing a spatially explicit representation of the export influence zone that supplements the scalar OMR metric (Reclamation 2025b).

These tools share a common limitation: they operate primarily as regression-based or lookup-table approaches calibrated to historical observations and do not capture the full mechanistic complexity of tidal hydrodynamics in the Delta.

Independent Reviews

The 2025 National Academies of Sciences, Engineering, and Medicine (NAS) review of the Long-Term Operations of the CVP and SWP provided an independent evaluation of the scientific basis for current regulatory frameworks and management tools (National Academies of Sciences & Medicine 2025). The NAS panel identified fundamental limitations in the use of OMR flow as a management target, noting that it is an index-based scalar that does not represent tidal advective-dispersive transport processes, cannot resolve spatially variable fish distributions, and has limited predictive power for entrainment risk and survival outcomes across the full range of Delta hydrologic conditions. The NAS review recommended that management transition toward more mechanistic, spatially explicit approaches grounded in habitat-based understanding of fish behavior and hydraulics.

The Delta Stewardship Council Delta Science Program (DSP) convened an Independent Peer Review Panel at the request of Reclamation and DWR to evaluate the annual loss accounting for Sacramento River winter-run Chinook salmon for Water Years 2024 and 2025 (Sturrock et al. 2026). The panel examined the decisions and operational conditions that contributed to the cumulative loss trajectories in both years, explored knowledge gaps and inefficiencies hindering real-time management, and recommended a fundamental shift from reactive to proactive, precautionary management, particularly during the critical February–March window when risk of exceeding loss thresholds is highest. Central to these recommendations is the need for tools that can rapidly assess hydrodynamic scenarios and the associated potential biological outcomes, enabling export decisions to be made before rather than after fish are salvaged.

3. Methodology

Dataset

In comparative analyses or planning analyses, DSM2 is often coupled with CalSim modeling (California Department of Water Resources 2023; Draper et al. 2004) where hypothetical hydrologic and operations scenarios simulated by CalSim are used as boundary conditions for DSM2 HYDRO. This coupling allows modelers to simulate hypothetical alternatives that cannot be shown by historical conditions, and the outputs of these coupled model runs are often treated as simulated data for further analyses.

Reclamation conducted a large-scale sensitivity study on the potential impacts of CVP and SWP operations over a wide range of hypothetical operations scenarios (hereinafter, OMR Sensitivity Study) with the CalSim-DSM2 coupling approach (Reclamation 2025c). Specifically, the OMR Sensitivity Study consists of 7 CalSim-HYDRO coupled simulations, spanning 100 years from October 1921 to September 2021 under the historical hydrologic conditions and seven different regulatory scenarios (Table 1). Note that this period is across 101 calendar years but aligns with 100 California water years, each of which runs from October 1 through September 30. Each CalSim-HYDRO coupled simulation is then associated with (1) 27,300 Particle Tracking Module (PTM) simulations resulting from surface-oriented particles released across 39 locations (Figure 1) and 700 timings (the first of every month from December through June over the 100 years), and (2) 396 ECO-PTM simulations with particle release occurring at the Sacramento River at Freeport across 396 timings (the first of every month from December through March over 99 years, skipping water year 1922). The outputs from the total of 191,100 PTM simulations and 2,772 ECO-PTM simulations form the simulated dataset for the responses of our study, whereas the outputs from the 7 CalSim-HYDRO simulations form the simulated dataset for the potential predictors. The simulated data provide great insight into how CVP and SWP operations could affect transport, entrainment, and salmonid responses over a wider range of conditions than has been observed in the field recently or would not be allowed under current regulatory conditions. The higher hydrodynamic variability in the simulated data also allows enhanced applicability of data-driven tools, which would otherwise be limited by the lower hydrodynamic variability in recent years.

Table 1. Alternative Regulatory Scenarios in the OMR Sensitivity Study

Regulatory Scenarios in The OMR Sensitivity Study	Regulatory Regime
L2020A	Dynamic management of OMR based on the 2024 Biological Opinions (National Marine Fisheries Service, 2024; U.S. Fish and Wildlife Service, 2024)
OMR2000	Fixed OMR management at -2,000 cfs from December through June
OMR3500	Fixed OMR management at -3,500 cfs from December through June
OMR5000	Fixed OMR management at -5,000 cfs from December through June
OMR6500	Fixed OMR management at -6,500 cfs from December through June
OMR8000	Fixed OMR management at -8,000 cfs from December through June
OMR9500	Fixed OMR management at -9,500 cfs from December through June

Key:
cfs = cubic feet per second
OMR = Old and Middle River flow

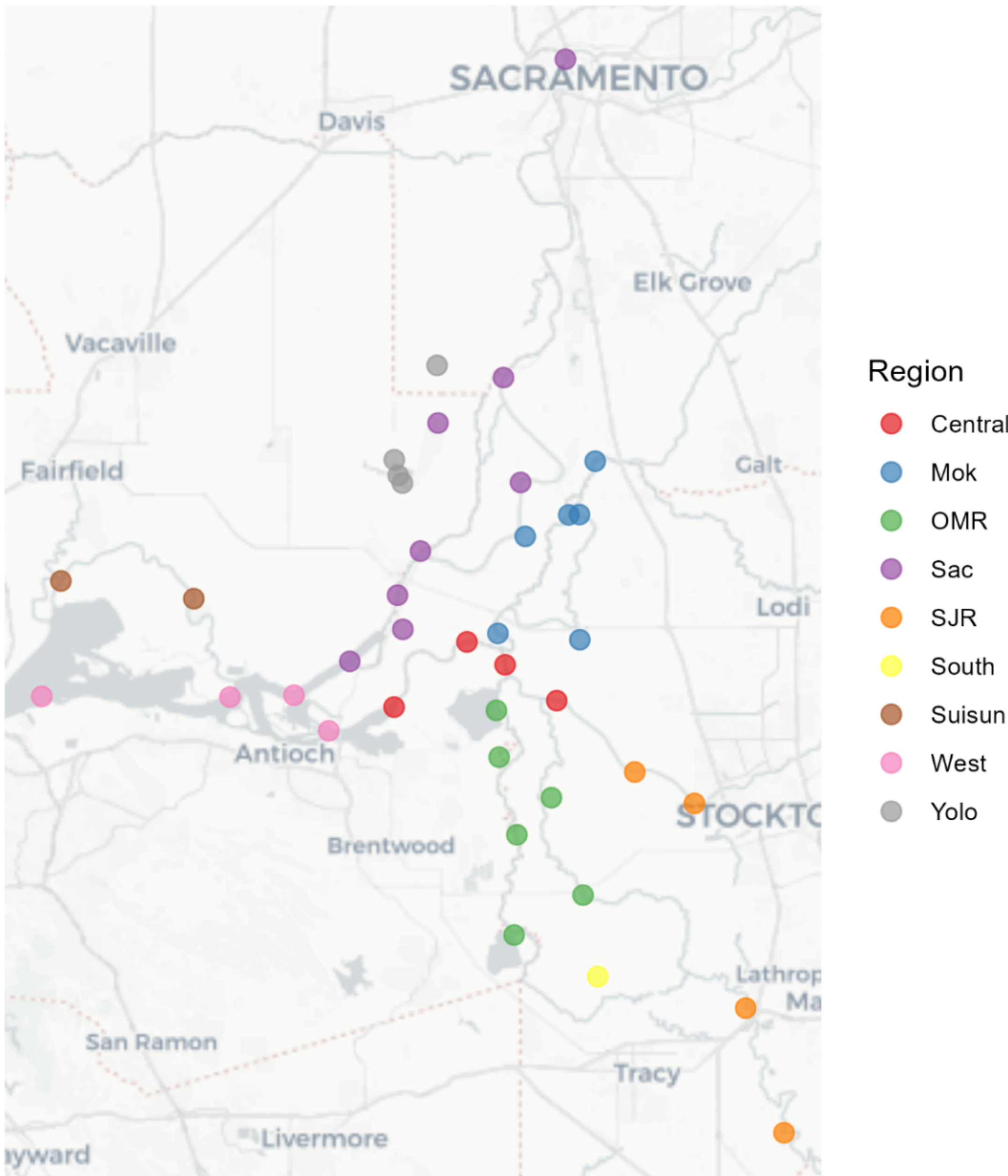

Figure 1. Particle Release Locations Color-Coded by Their Region Classification from the Old and Middle River Flow Sensitivity Study

General Modeling Framework

We adopted boosted regression tree as the main machine-learning structure to mine the simulated data because of this method's versatility in assimilating inputs of different types and scales (e.g., a mixture of categorical and numeric variables of different orders of magnitude), as well as its well-recognized predictive power. A boosted regression tree model is a machine-learning model that combines (1) regression trees, with recursive binary splits in the predictor space mapped to groupings in the response space, and (2) boosting, a sequential and additive ensemble learning technique to fit each model in the ensemble on the prior model's residual.

For all boosted regression tree models in this study, we combined 5-fold cross validation with either simple forward or simple backward variable selection process to simultaneously avoid overfitting and determine the set of predictors to be used in the predictive models. At the end of predictor selection, we built the final predictive model with the predictor set associated with the best cross-validation performance. Simple variable selection is preferred for two reasons. First, there are existing conceptual connections between the predictors and the responses based on domain knowledge, which informed our selection of the set of potential predictors for different responses prior to any data-driven variable selection (Table 2). Second, consistent with our research objectives, we favor model input parsimony and practical simplicity over the search for the best model. In other words, we will compare the marginal improvement in model predictive performance due to a predictor against the expected to obtain necessary data in practice, and factor this comparison into whether to include a predictor in the predictive model.

For reasons similar to the preference for simple variable selection, we determined the boosted regression tree parameters by simple trial and error starting from general, rule-of-thumb values. Parameters such as tree size (i.e., height limitation and node limitation of regression trees) and learning rate (i.e., the tradeoff between computational burden and the risk of overfitting) are typically important but often have a flexible optimal range instead of a precise optimal value. We stopped the trial-and-error process after noticing trivial marginal improvement in model performance.

Table 2. Potential Predictors from the Simulated Data to be Used for the Predictive Models of Different Responses

Potential Predictors	Acronym	Response Variable*	Conceptual Connection
Combined CVP and SWP Export (cfs)	EXP	P, E, H	Export is the primary driver of altered hydrodynamic regime in the Delta and is the most critical driver of entrainment.
San Joaquin River Flow at Vernalis (cfs)	SJR	P, E, H	San Joaquin River flow is the second largest boundary condition of Delta hydrodynamics, and it significantly determines the hydrodynamic regime in the south Delta, but is expected to be less informative in the north Delta.
Combined Flow in Georgiana Slough and through Delta Cross Channel Gates (cfs)	XGEO	P, E, H	Also referred to as the interior Delta flow, this combined flow plays a role in the transport from Sacramento River to the central Delta.
Sacramento River Flow at Freeport (cfs)	SAC	P, E, H	Sacramento River flow is the largest Delta inflow component and is a critical boundary condition for Delta hydrodynamics.

Potential Predictors	Acronym	Response Variable*	Conceptual Connection
Net Delta Accretion (cfs)	DICU	P	Net Delta accretion is a collective term consisting of small, localized boundary conditions of Delta hydrodynamics throughout the Delta. Despite its theoretical importance, it is difficult to measure or even estimate in practice, which goes against our research objectives. It is included here for localized entrainment response as a proof of concept to see whether its marginal benefits, if any, may outweigh its practical hurdle.
Combined East-side Flow: Mokelumne, Cosumnes, and Calaveras Rivers (cfs)	EAST	P, E, H	The east side flows are boundary conditions for Delta hydrodynamics and may play important roles under certain circumstances.
Flow in Mokelumne River Upstream of Its Confluence with Cosumnes River (cfs)	MOK	P, E	Mokelumne River flow is included here as a potential parsimonious surrogate of the east side flows for the spatiotemporally specific entrainment responses and the salmonid responses.

Note:

*: P stands for spatiotemporally specific entrainment responses, E stands for Sacramento-origin salmonid survival and routing responses, and H stands for spatially summarized entrainment responses.

Key:

cfs = cubic feet per second

CVP = Central Valley Project

SWP = State Water Project

ECO-PTM Emulator

CVP and SWP operations have the potential to affect Delta hydrodynamics, which in turn may affect the travel path, travel duration, and ultimately the survival of salmonids migrating from Sacramento River out of the Delta. To that end, we particularly focused on two ECO-PTM outputs: (1) combined through-Delta survival rate, which is the probability of an individual salmonid surviving from predators while it travels from Freeport towards Chipps Island integrated over the travel paths it could take, and (2) the interior Delta routing rate, which is the probability of an individual salmonid being routed into Georgiana Slough or the Delta Cross Channel. The former is the most direct ECO-PTM output linking flows and operations to salmonid survival in the Delta. The latter is relevant given that the routing into the interior Delta is associated with lower through-Delta survival for salmonids.

We adopted the general modeling framework (Section 3.2) with one minor adjustment to build boosted regression tree models that associate the two responses with subsets of predictions in Table 2. The minor adjustment was to bound the interior Delta flow at 4,000 cfs, and use the bounded flow as a candidate predictor. The reason for this adjustment is that the ECO-PTM simulated data included only the period of December through March, and during this period interior Delta flow was too closely related to Freeport flow to provide potential additional information, except when Delta Cross Channel Gates were open, which occurred in situations of lower flow. While it is not uncommon to have correlated predictors in tree-based models as surrogates for one another, we purposedly bounded the interior flow to force the model to only gather information from interior Delta flow in low flow situations and use Freeport flow in high flow situations.

The resulting models are essentially ECO-PTM emulators that allow users to estimate the two responses without the need of running ECO-PTM, thus overcoming the technical barriers and extending the models' applicability in practice. The responses are neither heavily skewed nor zero-inflated (Table 3), and thus we did not conduct any pre-processing for regression despite the fact that the responses are, theoretically speaking, bounded between 0% and 100%.

Table 3. Summary Statistics of the Salmonid Responses from the Simulated Data

ECO-PTM Response	Minimum	First Quartile	Median	Mean	Third Quartile	Maximum
Combined Survival (%)	23.0	38.2	47.1	47.8	58.3	68.6
Interior Routing (%)	6.6	9.4	16.0	14.5	18.5	26.3

Key:
ECO-PTM = Ecological Particle Tracking Module

PTM Emulator

CVP and SWP export operations have the potential to affect through-Delta transport and entrainment of particles, and particle entrainment has been used as a measure to assess the relative risk of entrainment of protected aquatic species in the Delta (especially smelt species). Hereinafter, we specifically refer to the combined entrainment into CVP's Jones Pumping Plant and SWP's Clifton Court Forebay (i.e., the export facilities) as entrainment.

Entrainment is a function of space (i.e., from where the particle is inserted and then transported to export facilities and entrained) and time (i.e., the time it takes for the transport process to take place). With practical considerations, we focused on two temporal scales: the 7-day entrainment and the 30-day entrainment. The former aligns with the weekly time scale of routine short-term operations management, whereas the latter aligns with the monthly time scale of mid-term to long-term operations planning and also represents a quasi-steady-state response. Having determined the temporal scales of interest, we accordingly define the spatial ranges to include all 39 particle release locations for the 30-day entrainment, and the 15 particle release locations (those nearest the export facilities) in the central and south Delta, OMR corridor, and San Joaquin River corridor for the 7-day entrainment (Figure 1). The smaller spatial range for the 7-day entrainment is to account for transport time; in 7 days very few particles from the more distant insertion points reach the export facilities.

Similar to the ECO-PTM emulators, we built PTM emulators by adopting the general modeling framework (Section 3.2) to associate the spatiotemporally specific entrainment responses (i.e., either 7 or 30 days after release at a given location) with subsets of predictors in Table 2. We included the combined export and San Joaquin River Delta inflow as default predictors for all candidate predictor sets due to their proven significance regarding entrainment at the export facilities. The particle release location was also included as a default categorical predictor to capture the differences among locations. Although it was a predictor from the machine learning aspect, in practice the particle release location would be a management parameter set by the model user, e.g., based on the habitat to evaluate. Unlike the case of the ECO-PTM emulators, some of the entrainment responses had skewed distributions and were inflated at either the lower or upper bound, warranting proper pre-processing. However, common data transform methods for percentage or probability, such as logit or arcsine transform, would also alter the scale of the regression error and make it challenging to cross-reference against the responses themselves. To address this issue, instead of transforming the responses, we let the model yield unbounded outputs, but we customized the model fitting loss function to evaluate bounded outputs. In other words, we did not penalize the model during training for making out-of-bound predictions, and we bounded the model outputs via post-processing. This approach preserved the linear scaling between error and the responses, ensured bounded model outputs, and avoided unnecessary model fitting penalties around the upper and low bounds.

Hydraulic Footprints

The rich spatiotemporal context of entrainment responses provides great technical details but could be unwieldy when applied to management and regulations. To address this challenge, we developed summary metrics of the entrainment responses aiming to achieve three goals at the same time: (1) the metrics are intuitive and amiable to an audience without hydrodynamic expertise, (2) the metrics account for advective-dispersive transport but do not require detailed hydrodynamic inputs for calculation or prediction, and (3) the metrics summarize the spatial context of entrainment into one single value that is relevant for management or regulations. We hereby define these summary metrics as hydraulic footprints and introduce them in the following subsections.

Hydraulic Footprint #1: Entrainment Event Horizon

Entrainment risk generally decreases with distance from the export facilities especially along the Old and Middle River corridor. We hereby define our first hydraulic footprint, the entrainment event horizon, as the shortest distance from Clifton Court Forebay gates along the Old River and Middle River corridor to the spatial boundary (i.e., horizon) of the high-entrainment-risk zone (Figure 2). The entrainment event horizon includes an entrainment risk tolerance and the spatial extent of the risk. Their interplay provides a direct connection to management and regulation because the risk tolerance can, and ideally should, be dynamically informed by management strategies, regulatory constraints, and the spatial distributions of biotic and abiotic factors relevant to the species of interest. The spatial extent of the entrainment risk then represents the distilled information corresponding to that risk tolerance.

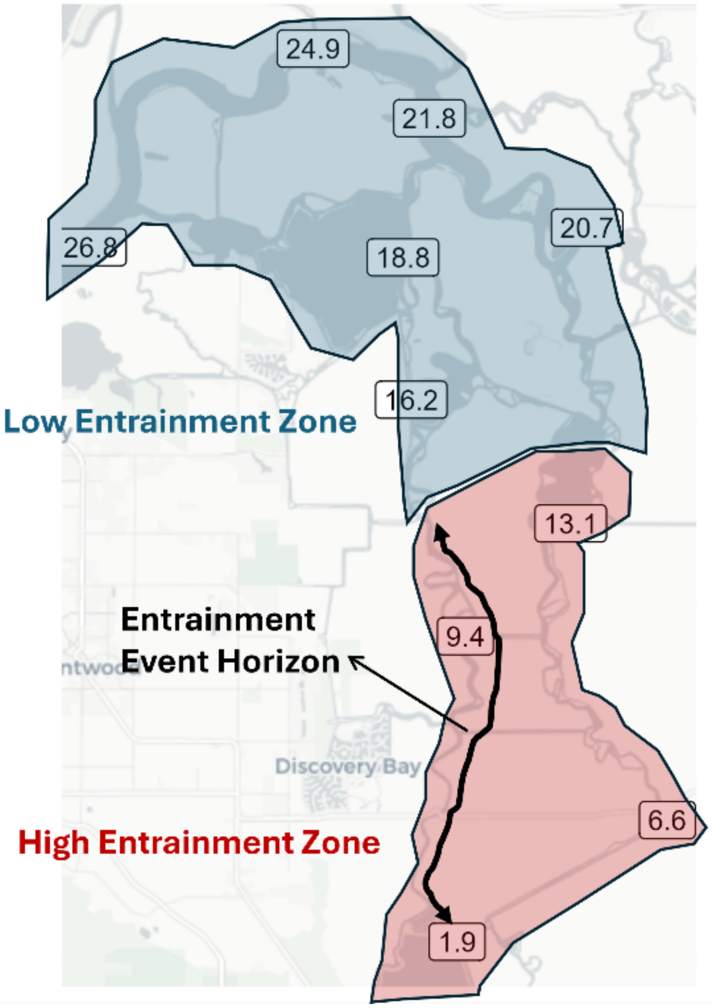

Note: particle release locations from the simulated dataset along Old and Middle River or in central Delta are annotated with their shortest distance (river miles) to Clifton Court Forebay gates.

Figure 2. Conceptual Illustration of the Definition of the Entrainment Event Horizon

To develop this quantitative metric, we first took a subset of the simulated data that included the 7-day entrainment responses at release locations within the central Delta and Old and Middle Rivers regions (Figure 1), and delineated their shortest paths to Clifton Court Forebay gates (i.e., the mileage in Figure 2). We chose this spatiotemporal configuration to correspond to the period of the autocorrelation among daily entrainment, and to focus on key locations of concern where representative levels of entrainment could occur within that short period. Second, we conducted linear interpolation between pairs of locations in Figure 2 to calculate the mileage corresponding to entrainment levels of 15% to 80% at 5% increments. This range was selected to encompass the most dynamic and management-relevant portion of the entrainment gradient while avoiding the statistical noise and asymptotic behavior typically found at extremely high or low entrainment levels. At higher entrainment thresholds, the entrainment event horizon is geographically restricted to areas in close proximity to the export facilities, whereas at lower thresholds the entrainment event horizon exhibits a much broader spatial footprint that is more sensitive to fluctuations in ambient Delta flows. The 5% increment was subjectively selected for less computational burden, assuming that these levels include, or are close enough to, most of the levels that may be of interest in practice.

Having developed the entrainment event horizon from the simulated dataset, we followed the general modeling framework in Section 3.2 to build a predictive model, with one minor modification where we included the target entrainment level (15% to 80% at 5% increments) as the default categorical predictor. Although it was a predictor from the machine learning aspect, in practice the target entrainment level would be more of a management parameter, similar to the particle release location parameter in PTM emulators. The predictive model would allow users to associate simple model inputs (Table 2) with the entrainment event horizon, without having to perform PTM modeling and linear interpolation.

Hydraulic Footprint #2: Entrainment Scale

Entrainment is inherently a spatiotemporal field because the response depends on the starting location of the subject of entrainment, either a passive particle or a fish, as well as on the time elapsed through the transport process. Ideally, we would like to look beyond the Old and Middle River corridor and summarize the complex spatiotemporal heterogeneity across the entire central and south Delta, but it could be challenging doing so through physics-based or analytical approaches while keeping the outcome intuitive and amiable to a wide audience. We therefore adopted a machine-learning-based approach to identify unique spatial patterns of entrainment risks and sort them into a discrete constructed scale system, which we hereby define as the entrainment scale.

To develop the constructed scale system, we first took a subset of the simulated data that included the 7-day and 30-day entrainment responses at several release locations within the central Delta, south Delta, San Joaquin River, and Old and Middle Rivers regions, and regrouped them into data views. In machine-learning context, a data view is one particular perspective or representation of the data on the subject of interest, and a multi-view dataset is a dataset that includes data of different perspectives on the subject. Under the scope of this study, we regrouped the locations based on the similarity in the statistical distribution of entrainment responses to determine the spatial views (Figure 3), and then we further broke down each spatial view into two temporal view, one with 7-day and the other with 30-day entrainment, resulting in 12 spatiotemporal views. The multi-view setup provided the basis to separately evaluate entrainment in different local areas as well as in near-term transient state versus quasi-steady state.

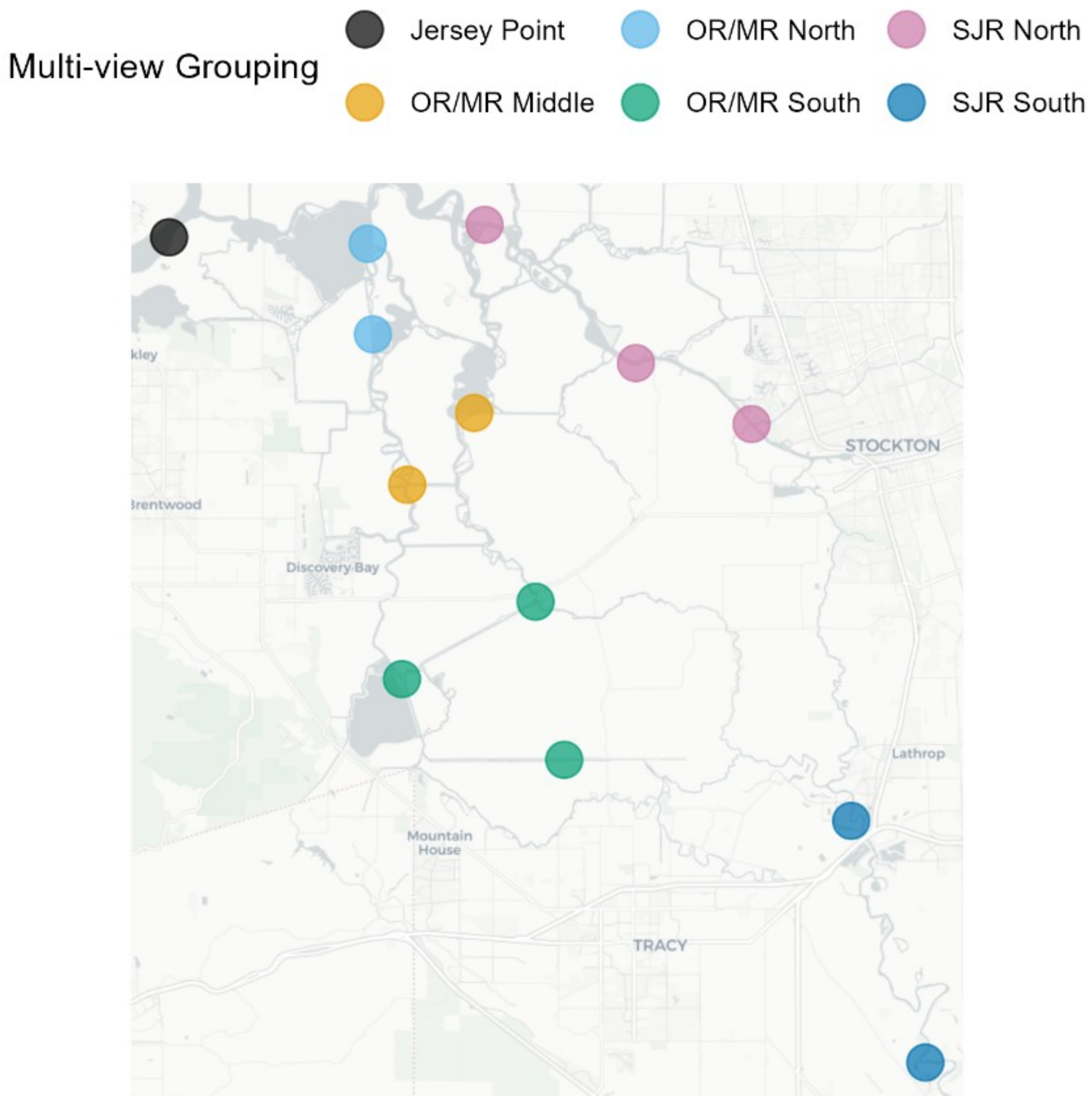

Figure 3. Map of Spatial Data View Grouping of Particle Release Locations

With the multi-view dataset, we then applied a coupled clustering algorithm, consisting of a single-view (i.e., weighing every view equally) approximate spectral clustering process (John et al. 2019) followed by a multi-view (i.e., each view contributes differently) k-means cluster aggregation process (Godichon-Baggioni et al. 2020), to yield 15 clusters. Every cluster represented a distinct pattern of entrainment, and they were sorted by their respective overall entrainment risk to make a constructed scale from 1 to 15. The number of discrete scales was chosen subjectively to balance the level of detail with both the noise in the data and the perceived complexity by an audience without machine-learning expertise.

We built the predictive model of the entrainment scale by simply coupling the PTM emulator (Section 3.4) with the k-nearest-neighbor algorithm (i.e., sorting of spatial entrainment patterns based on similarity), instead of following the modeling framework in Section 3.2. This was because the entrainment scale was categorical, ordered, and fuzzy, so it could accommodate uncertainties in entrainment such as those from the PTM emulator, but might be challenging to model with our general framework. In effect, the predictive model is equivalent to the PTM emulator with a post-processing step, and it would similarly allow users to associate simple model inputs (Table 2) with unique spatial entrainment patterns without having to go through PTM modeling.

Demonstration of Applicability

The aforementioned tools, including the emulators and the hydraulic footprints, were built with practical applications in mind, as they are expected to facilitate various analyses on the effects of CVP and SWP operations on hydrodynamic risk factors that affect entrainment and salmonid responses. To demonstrate that applicability, we conducted two example analyses, explained in detail in the following subsections.

Hindcast Analyses

We conducted hindcast analyses by first estimating the entrainment responses, salmonid responses, and hydraulic footprints using historical daily flow and export data from the DAYFLOW database. The hindcast spanned from water year 1984 through 2025 (i.e., from October 1st, 1983 to September 30th, 2025). Note that the hindcast values should not be misinterpreted as contemporary daily records, but rather the expected outcomes should those daily conditions have continued for a period of time (for transport to take place).

Through-Delta Survival

We compared the hindcast ECO-PTM emulator survival estimates with historical observed salmonid survival. We retrieved acoustic tag data of hatchery released Chinook Salmon and Steelhead from water year 2018 through 2025 from CalFishTrack (National Oceanic and Atmospheric Administration n.d.) to estimate observed survival. CalFishTrack reports results from acoustic tag studies and computes through-Delta survival using a Cormack-Jolly-Seber model. For each study-release group combination, we associated the calculated survival rate with the time period from the first arrival detected at Tower Bridge or the I-80/I-50 Bridge in Sacramento (whichever was earliest) through the last detection at Benicia. The two locations captured the ranges of ECO-PTM simulated outmigration from Freeport to Chipps Island. Release groups with zero survival (i.e., with more than one fish passing Tower Bridge or the I-80/I-50 Bridge but no survival to Benicia) were associated with their Delta entry dates. The main purpose of this comparison was to provide an additional piece of evidence of the applicability of the ECO-PTM emulators.

Entrainment at The Export Facilities

We conceptually assumed that the tidal advective-dispersive transport, which could be captured by the hydraulic footprints or the PTM emulator, is a necessary but insufficient condition for prediction of entrainment. To test this assumption, we compared the hindcast hydraulic footprints against the historical entrainment at CVP and SWP export facilities. We retrieved salvage data from SacPAS (University of Washington n.d.) on Chinook Salmon and Steelhead, and then added the expanded salvage to the calculated loss to estimate the total historical entrainment (California Department of Fish and Wildlife 2018). This processing was needed to take into account that the CVP and SWP fish facilities had different processes for sampling and salvaging, as well as the differences in ungauged, estimated facility loss (e.g., loss in the Clifton Court Forebay). To match the physical meaning of particle entrainment as close as possible, the total amount of fish that entered the export facilities included both the fish that were salvaged at the fish facilities and the fish that were lost (e.g., due to predation). Due to the lack of well-supported estimates of losses (the behavioral-based guidance used for salvage does not work well on weak swimmers), we did not analyze the historical entrainment of Delta Smelt and Longfin Smelt even though salvage data were available.

The main purpose of this comparison was to evaluate the potential extent to which species entrainment could have been explained by hydrodynamics had we had better hydrodynamic indicators, such as particle entrainment or hydraulic footprints. We recognize that the historical salvage data involve much more than just hydrodynamics, such as field sampling, process assumptions, and biological or environmental confounding factors, all of which contribute to uncertainties and are out of the scope of this study. Nonetheless, this hindcast analysis provides a re-evaluation of the combined magnitude of those uncertainties by more comprehensively accounting for the hydrodynamic effects.

Inverse Modeling Analysis

From the management or regulation perspective, users of our tools may be more interested in determining the level of flow or export that is associated with a specified response, i.e. the inverse application of our tools. We took a subset example period out of the hindcast analysis and conducted an inverse analysis, where we quantified the marginal effect of changes in flow or export on the entrainment responses and hydraulic footprints. The inverse analysis demonstrates a potential paradigm shift as we could design alternative operations based directly on hydrodynamic-informed entrainment risks, rather than indirectly on averaged flows. This potential paradigm shift signifies a corroborated connection from the outcomes of regulations (e.g., alternative operations) to the purposes of regulations (e.g., protecting listed species in the Delta).

4. Results

ECO-PTM Emulator

The out-of-sample root mean squared error (RMSE) was used as the indicator of the predictive performance of candidate predictor sets form the simple forward selection process (Figure 4). Sacramento River Flow at Freeport was found to be the most dominant single-predictor for ECO-PTM responses, while export appeared to be the worst single-predictor. This could be attributed to focus in ECO-PTM on the migration route from Freeport towards Chipps Island (Wang et al. 2024) and is consistent with prior findings on the limited effects of export on survival (D. J. Hance et al. 2022).

As the simple forward selection proceeded, we found that for interior routing the predictor combination of Freeport flow, Mokelumne flow, and interior Delta flow yielded the lowest error and hence was determined the best predictor set. For survival, all predictor sets with 3 or more predictors had similar predictive performance, so we determined the most parsimonious set, with Freeport flow, Yolo Bypass flow, and Mokelumne flow, as the best predictor set. The detailed cross-validation performance of the best predictor sets is shown in Figure 5, indicating negligible bias and heteroscedasticity of predictive error against data.

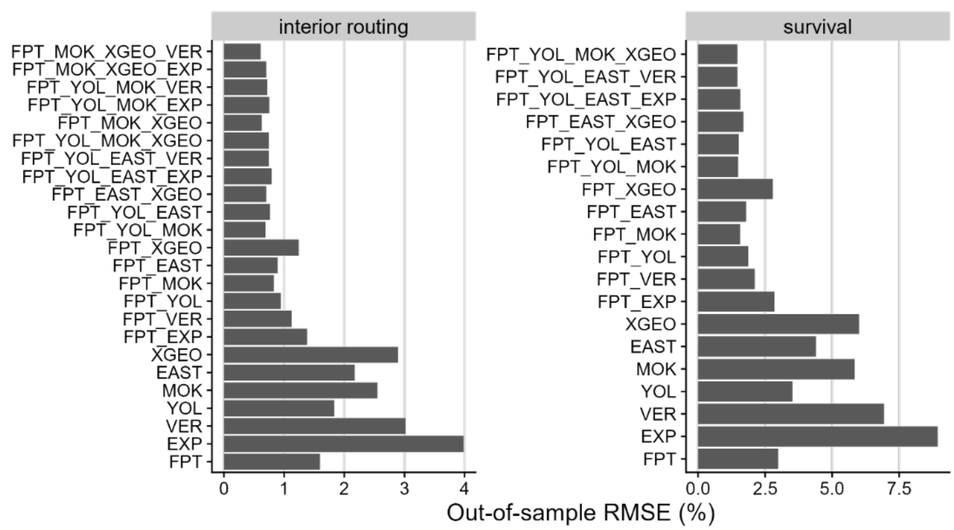

Note: Predictor sets are annotated with acronyms specified in Table 2.
Key:
ECO-PTM = Ecological Particle Tracking Module
RMSE = root mean squared error

Figure 4. Out-of-Sample RMSE of the Candidate Predictor Sets for the ECO-PTM Interior Routing and Survival Emulators from the Simple-Forward Predictor Selection Process

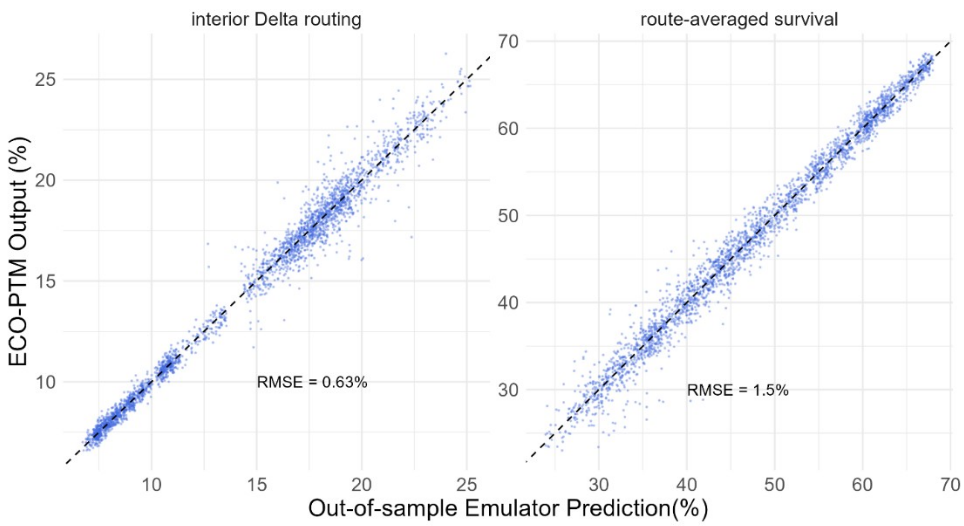

Note: The dashed line is the 1:1 line symbolizing perfect match between ECO-PTM and the emulators.
Key:
ECO-PTM = Ecological Particle Tracking Module

Figure 5. Scatter Plots of the Cross-Validation Results for the Two Best Predictor Sets for ECO-PTM Responses

To evaluate the mechanistic explanation for the best predictor set, we inspected the correlation between ECO-PTM responses and flows and found an interesting phenomenon in low-flow situations. While the correlation between flows and survival is mostly monotonic (Figure 6 top row), the correlation between flows and interior routing shows inflection from very low flow to moderately low flow (Figure 6 bottom row), as well as more separation of points depending on Delta Cross Channel Gate position. Cross-referencing Figure 6 to Figure 5, the inflection explains the bimodal distribution of interior routing and the higher complexity in low flow, high interior Delta routing situations likely contributed to the minor heteroscedasticity. This finding adds on top of prior studies which showed that the probability of routing into the interior Delta could decrease with Delta inflow (Perry et al. 2018) and that flow has a positive effect on survival in the interior Delta (D.J. Hance et al. 2022). The inflection is not seen for survival, indicating that while complication around interior Delta routing exists in low flow situations, that routing per se may not have a significant effect on survival when survival is low overall.

In contrast, combined export shows poor correlation with interior Delta routing, and weak positive correlation with survival when the interior routing percentage is moderate to high (Figure 7), and the direction of the poor correlation goes against a general conceptual belief that more export results in more impacts on survival and routing. This is likely due to the mechanistic correlation between export and Delta inflows, rather than that between export and survival. Even though the simulated data came from model simulations over a wide range of regulatory regimes for the Old and Middle River corridors, higher simulated export still generally occurred with higher Delta inflows to maintain mass balance at the Delta macro scale, because various other regulations were still in place. Under that macro scale, the effect of export on Sacramento-origin salmonids, if any, could be small compared to those of Delta inflows or DCC operations (which is accounted for by the interior Delta flow in the model). From the perspective of model simulations, if one changes export in ECO-PTM simulations while keeping all other boundary conditions the same, one may observe differences in the simulated survival. However, in our simulated data these differences were volatile and we could not draw a statistically sound conclusion on the marginal effect of export with our modeling framework.

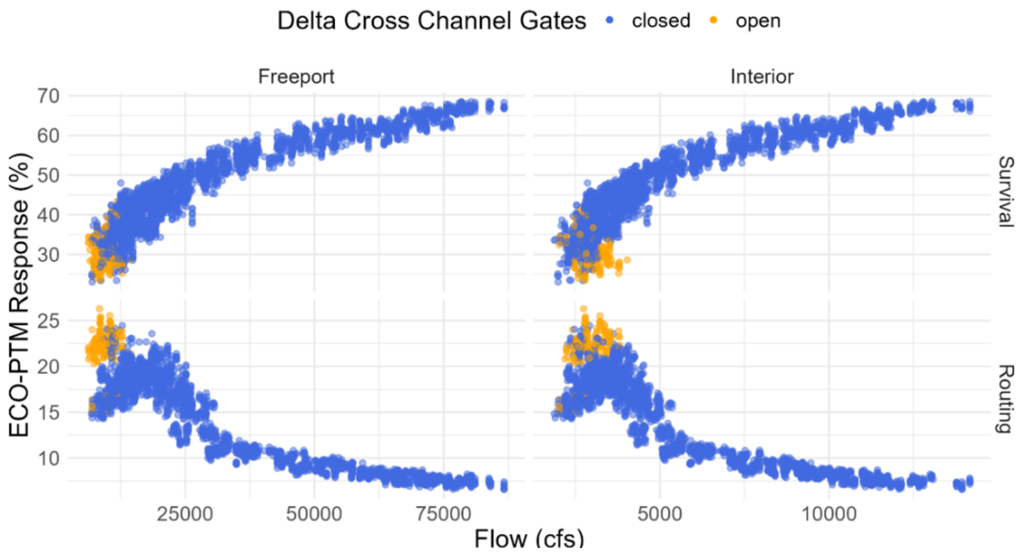

Notes: Freeport and interior Delta flow, left and right respectively. Route-averaged survival and interior Delta routing, top and bottom respectively.

Key:

ECO-PTM = Ecological Particle Tracking Module

Figure 6. Scatter Plots of Predictors Against ECO-PTM Responses

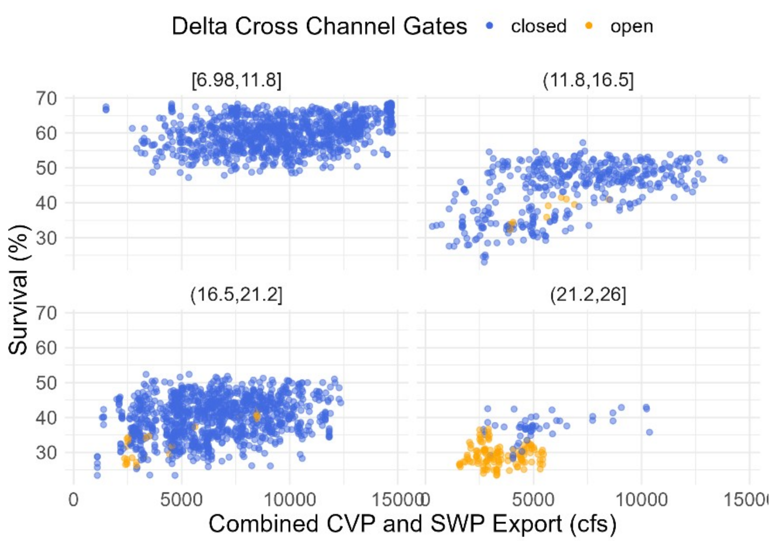

Note: For example, (11.8, 16.5) means larger than 11.8% but smaller or equal to 16.5 %.

Key:

ECO-PTM = Ecological Particle Tracking Module

Figure 7. Scatter Plot of Combined Export Against ECO-PTM Simulated Survival, Categorized by Quartiles of Interior Delta Routing Annotated in Brackets

PTM Emulator Performance

We similarly used out-of-sample RMSE as the performance metric for the simple forward prediction selection. The significant reduction in RMSE by adding any predictor to the benchmark set indicates that although export and Vernalis flow are the two most critical driving forces, they are not enough to explain the transport and entrainment of particles originating from further away such as the central Delta, around the Mokelumne River, or along the San Joaquin River. As the simple forward selection proceeded, we found that for both the 7-day and 30-day entrainment responses (Figure 8 and Figure 9 respectively), all predictor sets with 3 or more additional predictors performed fairly well, with subtle improvements sporadically distributed over regions and predictor sets.

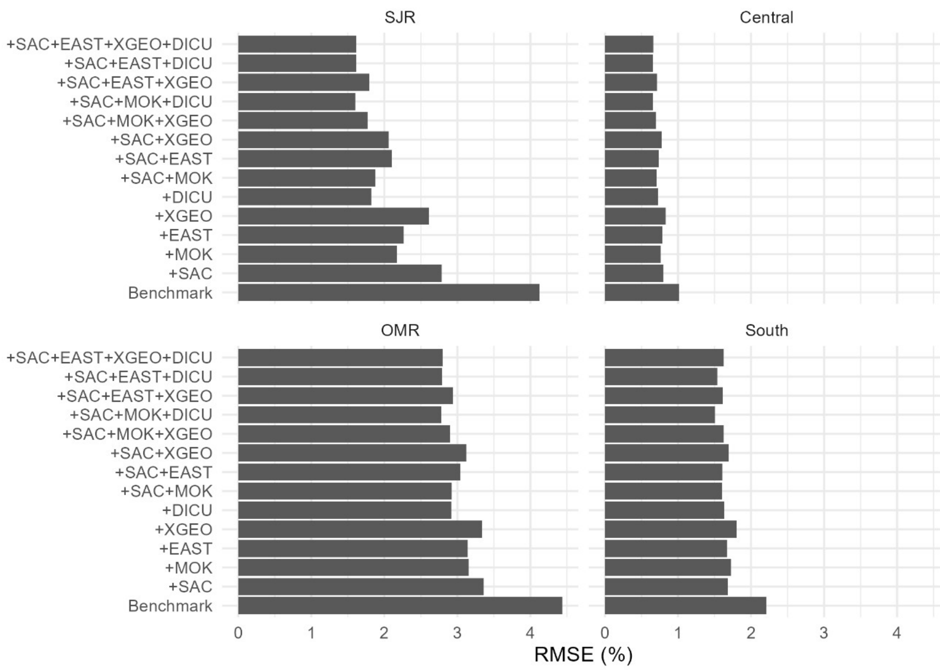

Note: The benchmark set includes the default predictors (export, Vernalis flow, location), and the other predictors sets are annotated by the additional predictors to the benchmark, with acronyms specified in Table 2.

Key:

PTM = Particle Tracking Module

RMSE = root mean squared error

Figure 8. Out-of-Sample RMSE of the Candidate Predictor Sets for the PTM 7-day Entrainment Emulator by Region (Figure 1)

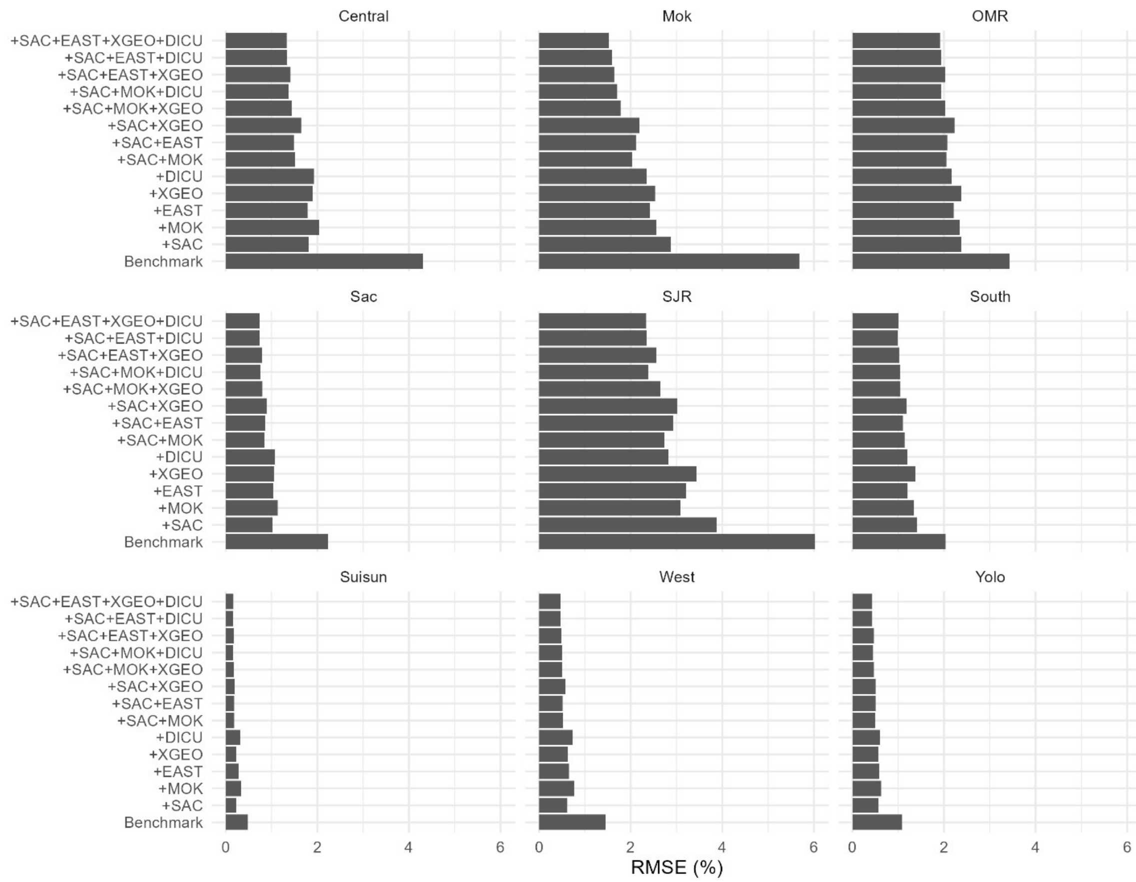

Note: the benchmark set includes the default predictors (export, Vernalis flow, location), and the other predictors sets are annotated by the additional predictors to the benchmark, with acronyms specified in Table 2

Key:

PTM = Particle Tracking Module

RMSE = root mean squared error

Figure 9. Out-of-Sample RMSE of the Candidate Predictor Sets for the PTM 30-day Entrainment Emulator by Region (Figure 1)

We subjectively determined the predictor set with Freeport flow, eastside Delta inflow, and the interior Delta flow on top of the default predictors (export, Vernalis flow, and location) to be the best set. This choice was based on balancing the marginal improvement in predictive performance with the availability and uncertainty of a predictor in practice. For example, because eastside Delta inflows are reasonably available, we decided to have the combined eastside inflow over only Mokelumne flow for the marginal improvement in the Mokelumne region (Figure 9). In contrast, we determined that the marginal improvement provided by the Delta consumptive use predictor did not outweigh the associated uncertainty in the predictor itself, because in real-time operations the consumptive use is often estimated by a fixed timeseries and based on the precipitation at one station in Stockton (California Department of Water Resources n.d.), and therefore it was not included in the best set of predictors. The detailed cross-validation performance of the best predictor set for the 7-day and 30-day entrainment is shown in Figure 10 and Figure 11 respectively. Despite a few outliers, overall there is no bias or heteroscedasticity of predictive error against data.

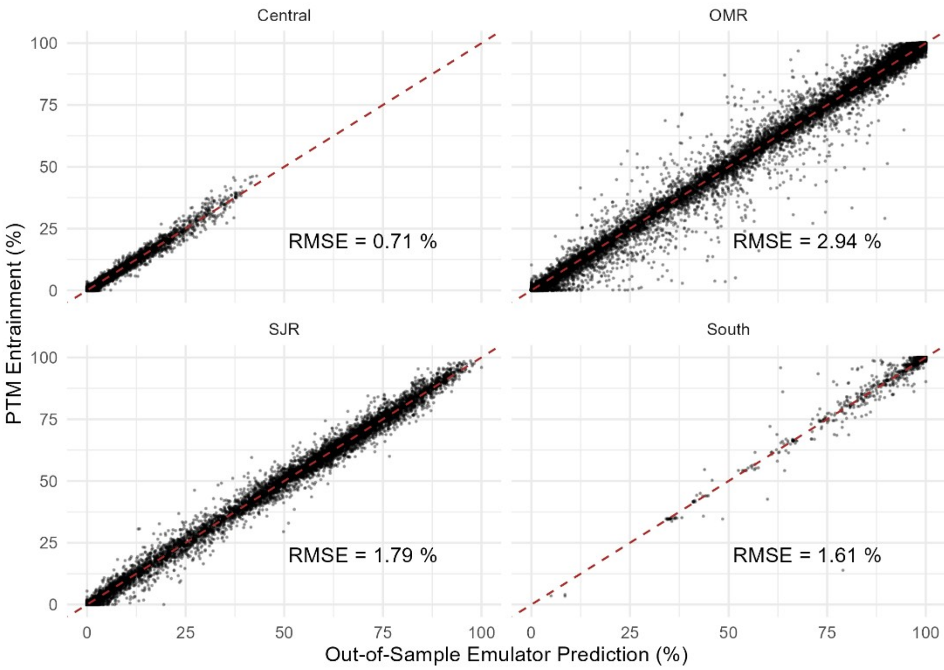

Note: The dashed line is the 1:1 line symbolizing perfect match between PTM and the emulator.
Key:
PTM = Particle Tracking Module

Figure 10. Scatter Plots of the Cross-Validation Results, by Region, for the Best Predictor Set for PTM 7-day Entrainment

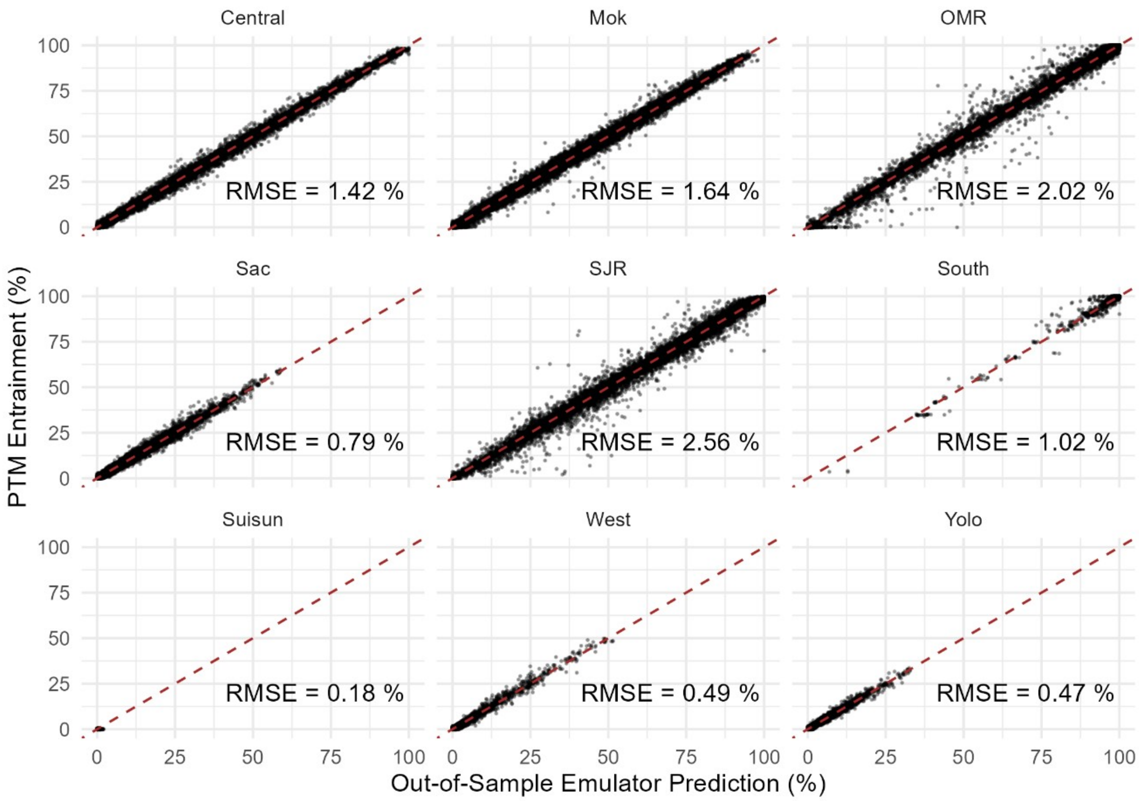

Note: The dashed line is the 1:1 line symbolizing perfect match between PTM and the emulator.
Key:
PTM = Particle Tracking Module

Figure 11. Scatter Plots of the Cross-Validation Results, by Region, for the Best Predictor Set for PTM 30-day Entrainment

Hydraulic Footprints

Entrainment Event Horizon

The entrainment event horizons were calculated from the simulated data following the spatial linear interpolation (Section 3.5.1). Figure 12 shows an example of the distribution of 15% event horizon (i.e., the spatial extent of the high entrainment risk zone where "high risk" is defined as 15% or more entrainment) with export and Vernalis flow, the two most critical components in operations and export management for species protection.

The entrainment event horizon provides a concise summary of underlying hydrodynamics, where the marginal effect of a unit change in export depends on Vernalis flow and also on export itself. For example, when Vernalis flow is above 20,000 cfs, entrainment risk is generally constrained to the immediate vicinity of the export facilities, except when export is at full capacity and Veranlis flow is barely above 20,000 cfs. Once Vernalis flow drops below 20,000 cfs, the tradeoff between export and Vernalis flow starts to dynamically manifest, as indicated by the contours of different shapes and slopes.

The spatial context is also summarized where one can incorporate domain knowledge on the species to reference key locations (e.g., regulatory locations or known species habitat areas, etc.) against hydrodynamics. While the 15% horizon is provided here as an example, the targeted risk level itself lends an additional layer of added information, where domain knowledge could be integrated in a quantitative way to inform the degree of export restriction.

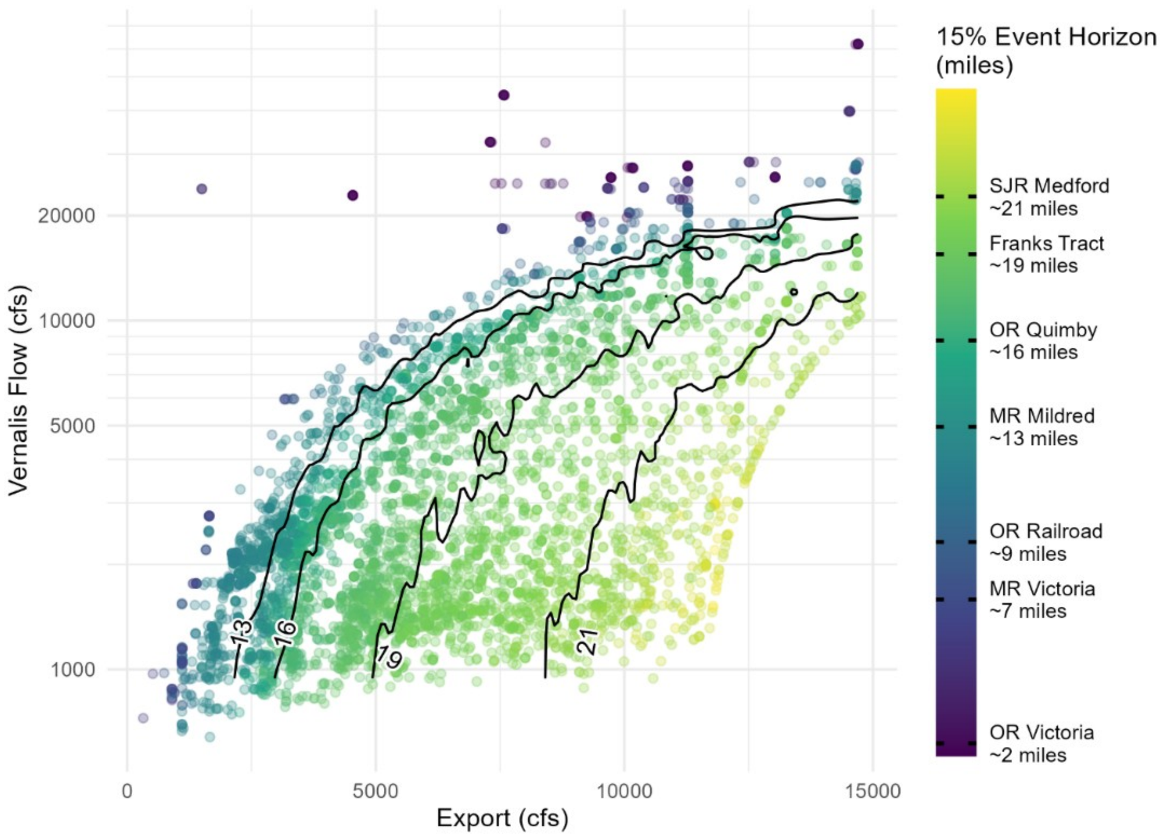

Notes: Distances from Clifton Court Forebay gates to key particle release are annotated for reference with the following abbreviation: OR = Old River; MR = Middle River; SJR = San Joaquin River; Victoria = Victoria Canal; Railroad = Railroad Cut; Mildred, Quimby, and Medford refer to Delta island names; contours at select distances are shown for references

Figure 12. Scatter Plots of Combined Export with Vernalis Flow (log-scaled for visibility), Color-Coded by the 15% Entrainment Event Horizon

We followed the general modeling framework with a simple backward prediction selection process (Section 3.2) to establish the predictive model for the entrainment event horizon. We started with all the predictors for the hydraulic footprints listed in Table 2, and progressively removed one predictor at a time to see whether there was a change in the cross-validation performance. The order of predictor removal was informed by the predictor gain during training (i.e., how much training error was reduced due to a predictor). The backward selection process resulted in a 5-predictor set including the target entrainment level, export, Vernalis flow, eastside Delta inflows, and interior Delta flow. Including Freeport flow in addition to those five predictors did not improve the out-of-sample predictive performance, which emphasized that the routing of water through the interior Delta (Georgiana Slough and the Delta Cross Channel) is a more proximal driver of entrainment risk in the Old and Middle River corridor than the Delta inflow at Freeport. This distinction allows the model to remain sensitive to Delta Cross Channel gate operations and localized hydraulic shifts captured within the interior Delta flow.

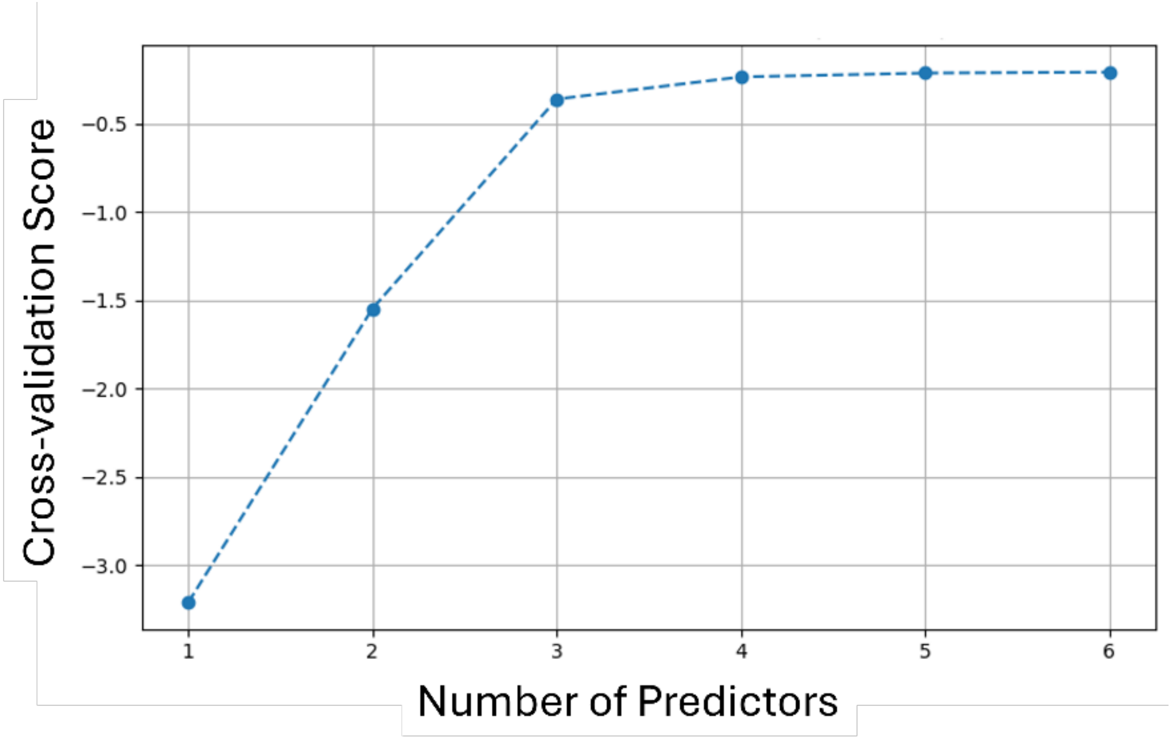

Note: The higher the cross-validation score the better, and if two scores are the same the smaller predictor set is preferred.
Key:
RMSE = root mean squared error

Figure 13. Cross-Validation Score (Negative Out-of-Sample RMSE in River Miles) of the Different Predictor Sets for Entrainment Event Horizon Predictor Model

The cross validation showed a high level of accuracy without significant bias or heteroscedasticity (Figure 14). This stability indicated model reliability even under edge-case hydrologic conditions, such as extreme droughts or high-flow pulse events. With this predictive model we not only bridged the gap from hydrology (i.e., the flow and export inputs) to hydrodynamics (i.e., the entrainment response governed by the tidal advective-dispersive transport in the Delta), but also took it one step further to management and regulation strategies, with which operational restrictions could be determined based on the spatial context of entrainment risk rather than averaged flows.

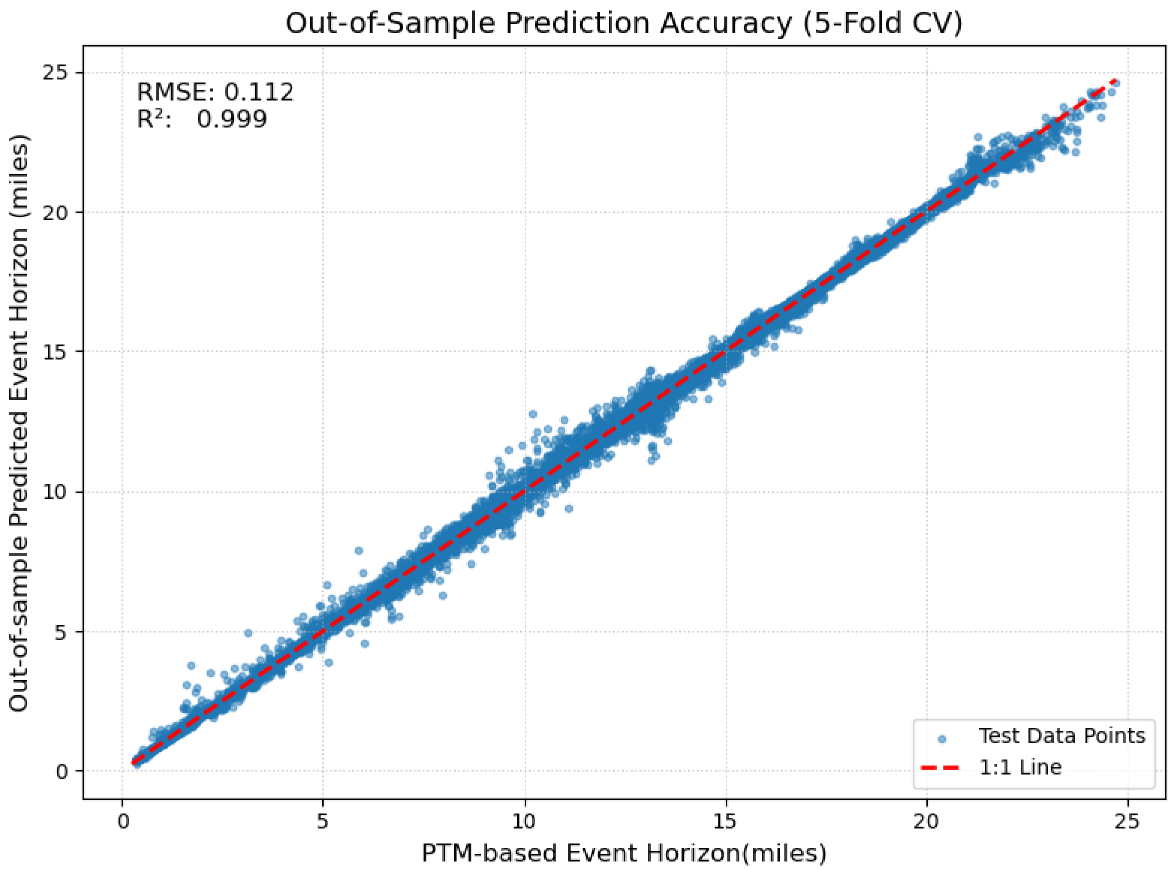

Note: The red diagonal dashed line is a 1:1 line indicating perfect match.

Figure 14. Scatter Plots of the Cross-Validation Out-of-Sample Predicted Entrainment Event Horizon from the Predictive Model Versus the Event Horizon from the Simulated Data

Entrainment Scale

The entrainment scale marked and sorted 15 distinct spatial patterns of entrainment by their respective overall entrainment risk. The entrainment scales themselves might not be as easily implementable as the entrainment horizon due to their discrete nature and thus relative lack of precision, but they offer great exploratory insights into a general assessment of the interplay between export and Vernalis flow.

We observed 3 unique ways in which entrainment patterns shifted with increased export and/or decreased Vernalis flow. This first and simplest one occurred when Vernalis flow was high, approximately above 20,000 cfs or above 95% of the historical flows, entrainment risk is highly constrained to the immediate vicinity of the export facilities (entrainment scale 1), but increased export would result in elevated entrainment (entrainment scale 2) from the more upstream insertion points in the San Joaquin River (Figure 15). Note that increased export had minimal effect on the entrainment risk along Old and Middle Rivers, indicating minimal interplay between the two and consistent with Figure 12 where the entrainment event horizon was kept within a few miles.

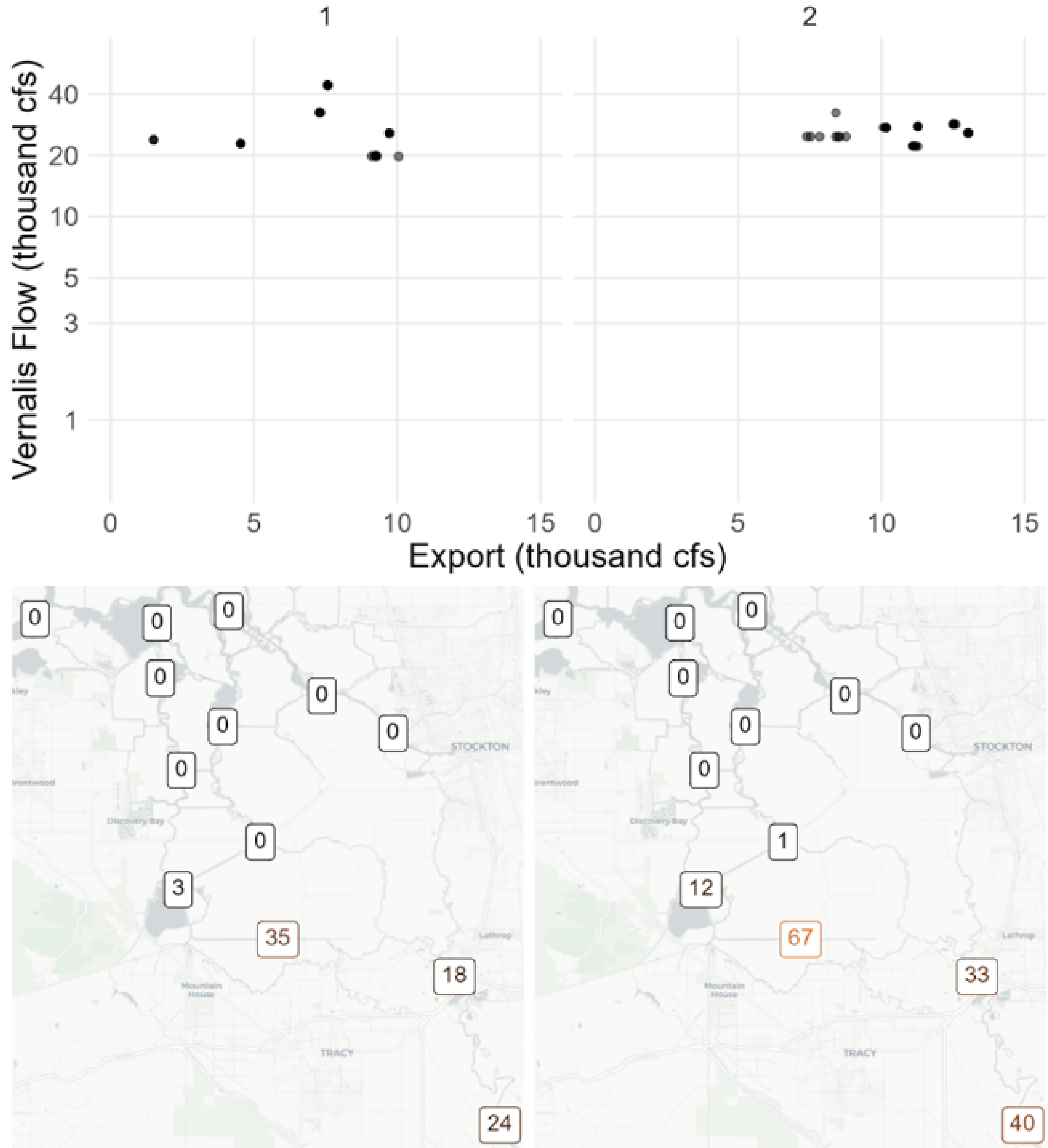

Note: Each box in the entrainment maps in the bottom row indicates the average percentage of particles entrained from that release location after 30 days, color-coded by degree of entrainment.

Figure 15. Scatter Plots of Export Against Vernalis Flow (log-scaled for visibility) by Entrainment Scales 1 and 2 (top row), and Their Associated Maps of Spatial Pattern of Entrainment Throughout Central and South Delta (bottom row)

At lower Vernalis flow, we observed the formation of the export-Vernalis interplay at entrainment scale 3, and as it progressed the relationship changed both in shape and in precision, indicating fuzzier marginal effects of both export and Vernalis in high-risk scenarios (Figure 16). These relationships roughly corresponded to the contours shown in Figure 12, and represented the majority of the data points in scenarios where Vernalis flow was neither dominant nor negligible. A related observation was that under these scenarios, the entrainment risk at Jersey Point remained low regardless of entrainment scale, indicating that Vernalis flow had enough balancing effect such that export was not exclusively pulling water from central or north Delta. This finding reveals why in some cases and in prior studies, the ratio of export to Vernalis flow or other south-Delta-focused flow metrics were potentially useful. Our results indicate that it is indeed feasible to maintain a similar level of entrainment, and even its spatial heterogeneity, by simultaneously manipulating export and Vernalis flow. However, the marginal effects of Vernalis flow or export were dynamically linked to the magnitudes of one another and were more complex than fixed ratios.

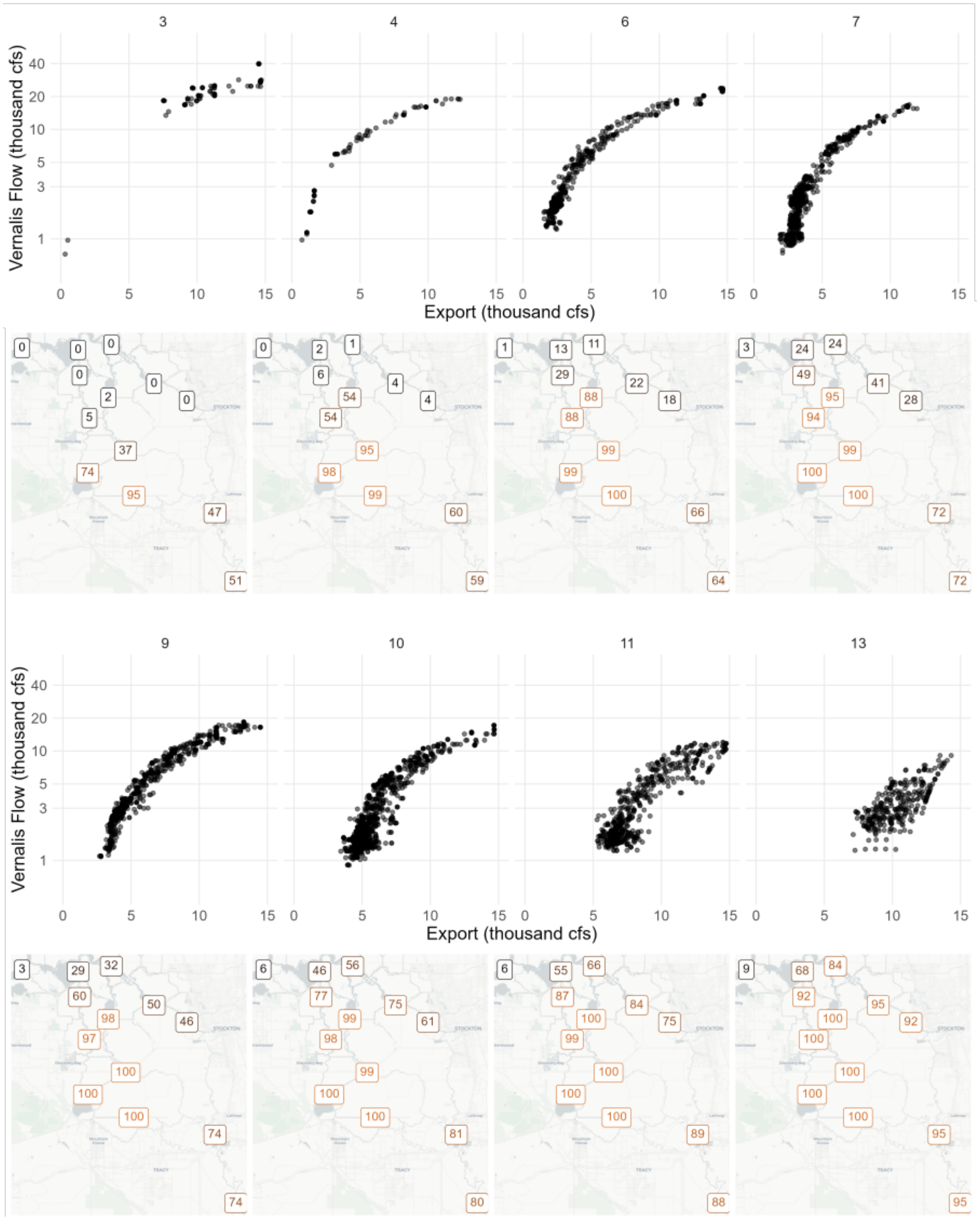

Note: Each box in the entrainment maps in the second and fourth rows indicates the average percentage of particles entrained from that release location after 30 days, color-coded by degree of entrainment.

Figure 16. Scatter Plots of Export Against Vernalis Flow (log-scaled for visibility) by Entrainment Scales 3 Through 7 (top row), 9 Through 11, and 13 (third row), and the Associated Maps of Spatial Pattern of Entrainment Throughout Central and South Delta (second and fourth row)

When Vernalis flow was low compared to export, the entrainment scales showed the third unique transition of entrainment patterns, where higher variability along the San Joaquin River was observed (Figure 17). The marginal effect of increased export became more significant in the upstream San Joaquin River, central Delta, and more visibly at Jersey Point. This was the only trend along which elevated risk at Jersey Point was observed, which was an indication of extended impacts of export beyond central Delta and might be important to species distributed further downstream.

Note: Each box in the entrainment maps in the bottom row indicates the average percentage of particles entrained from that release location after 30 days, color-coded by degree of entrainment.

Figure 17. Scatter Plots of Export Against Vernalis Flow (log-scaled for visibility) by Entrainment Scales 5, 8, 12, 14, and 15 (top row), and Their Associated Maps of Spatial Pattern of Entrainment Throughout Central and South Delta (bottom row)

Hindcast Analysis: Through-Delta Survival

The hindcast comparisons between the observed survival retrieved from acoustic tag studies and the estimated survival from the ECO-PTM emulator are shown in Figure 18 through Figure 23. The ECO-PTM emulator captured the trends in water years 2022 and 2023 well for Fall-Run (Figure 18), Winter-Run (Figure 20), and Spring-Run (Figure 21) Chinook salmon, where survival was consistently lower in 2022 and higher in 2023 despite the seasonal pattern. While the magnitude may not be perfectly matching, for all Chinook salmon the emulator also captured the trends of generally lower survival in water years 2020 and 2021, as well as the seasonal trend in water year 2025 (Figure 18 through Figure 22). Note that the observed survival values in Figure 22 were from studies without a specified run or with mixed runs (e.g., the hatchery-origin seasonal survival studies). An assumption we made for this comparison was that because the fish involved were all similar-sized taggable smolts, their interactions with the same environment would be similar rather than run-specific. Unlike Chinook salmon, the observed survival of steelhead appeared to be consistently higher than the emulator output (Figure 23), which could be attributed to the difference between juvenile Late-Fall-Run (the subject of the data ECO-PTM was calibrated against) and steelhead in their migration behavior and/or vulnerability to predators.

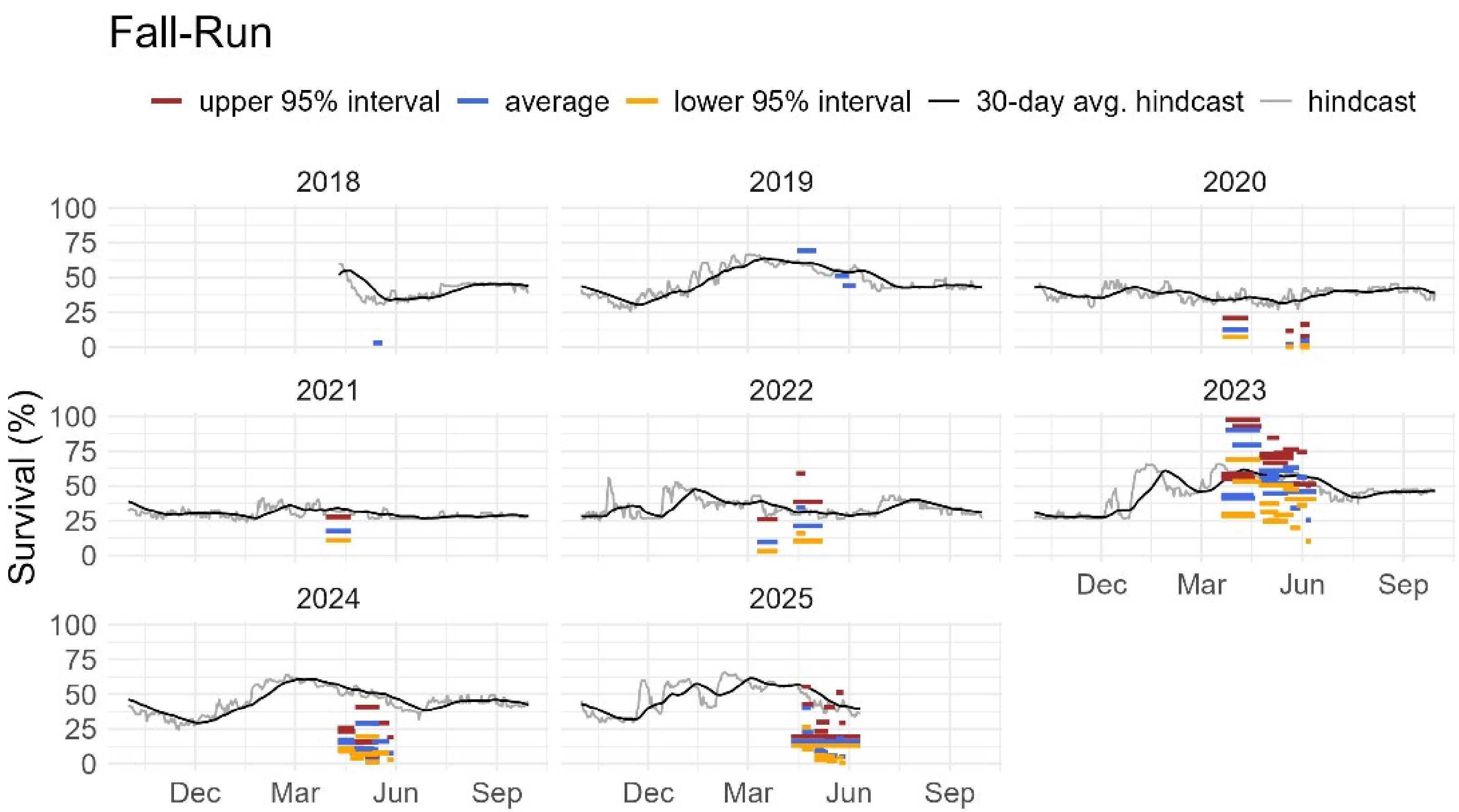

Note: Acoustic tag studies are shown as the average survival and 95% confidence interval for every study-release group combination and the ECO-PTM Emulator Hindcast Survival are shown as daily and 30-day running averages.
Key: ECO-PTM = Ecological Particle Tracking Module

Figure 18. Comparison Between the Observed Survival from Acoustic Tag Studies and the ECO-PTM Emulator Hindcast Survival by Water Year for Fall-Run Chinook Salmon

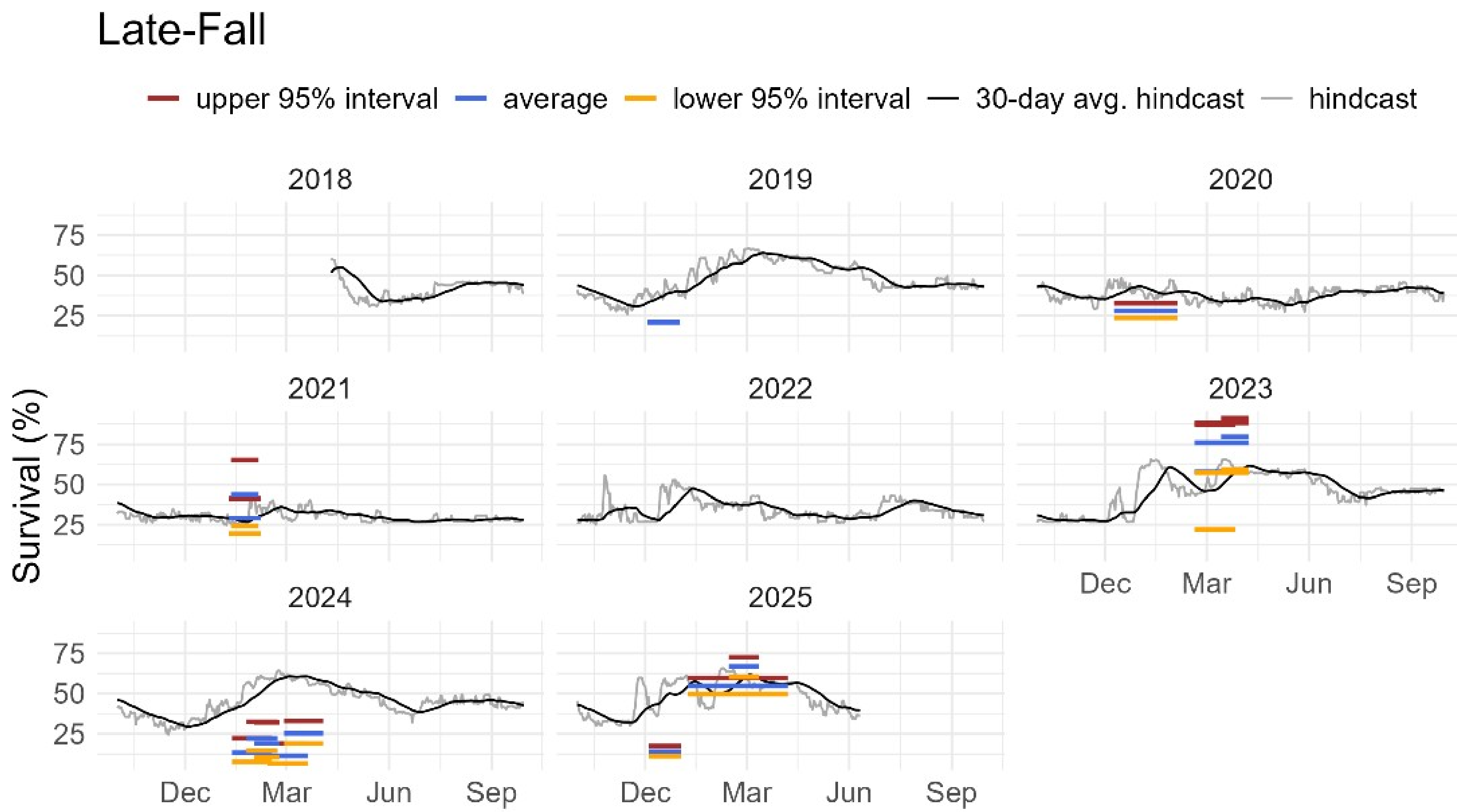

Note: Acoustic tag studies are shown as the average survival and 95% confidence interval for every study-release group combination and the ECO-PTM Emulator Hindcast Survival are shown as daily and 30-day running averages

Key: ECO-PTM = Ecological Particle Tracking Module

Figure 19. Comparison Between the Observed Survival from Acoustic Tag Studies and the ECO-PTM Emulator Hindcast Survival by Water Year for Late-Fall-Run Chinook Salmon

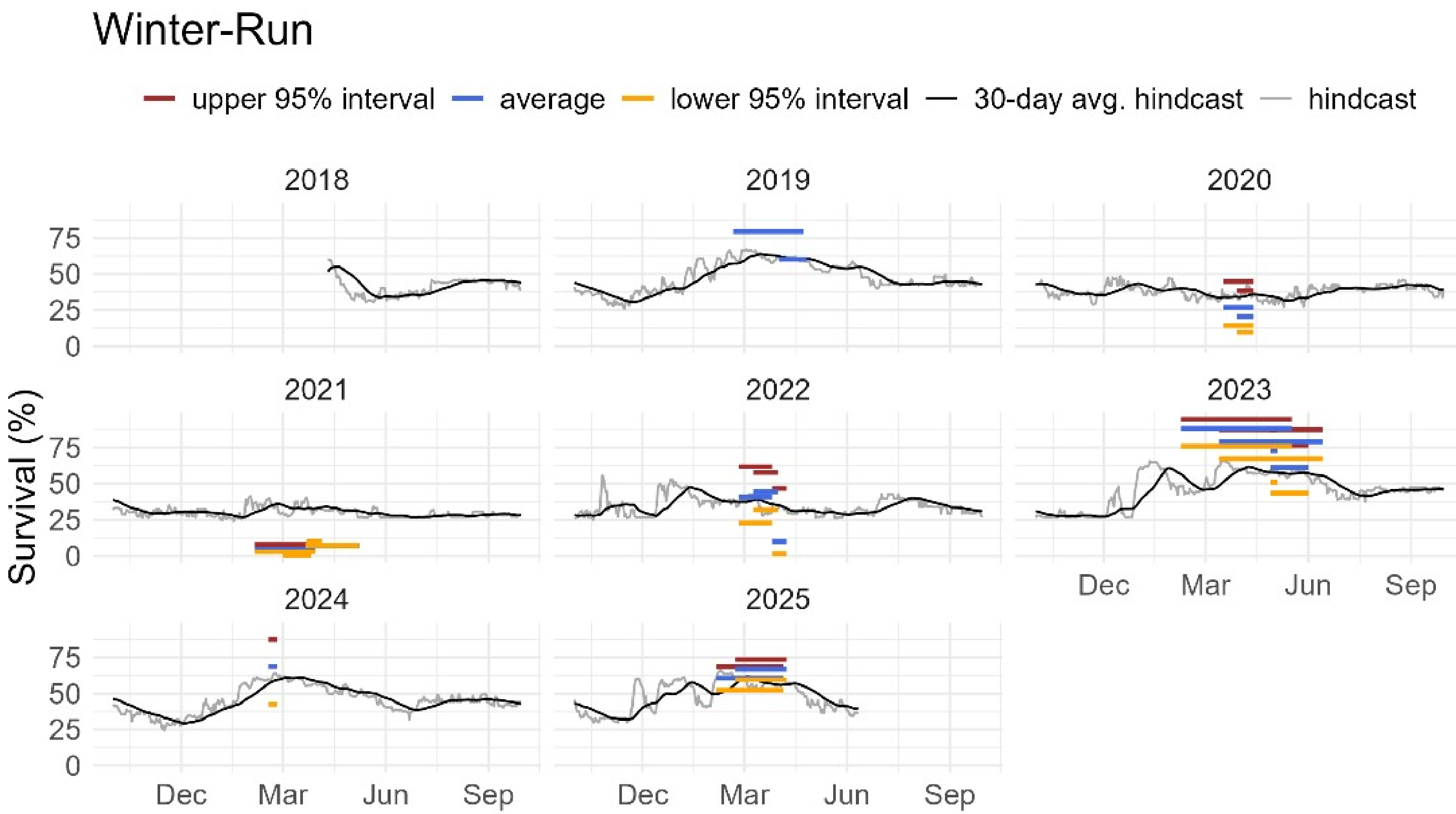

Note: Acoustic tag studies are shown as the average survival and 95% confidence interval for every study-release group combination and the ECO-PTM Emulator Hindcast Survival are shown as daily and 30-day running averages

Key: ECO-PTM = Ecological Particle Tracking Module

Figure 20. Comparison Between the Observed Survival from Acoustic Tag Studies and the ECO-PTM Emulator Hindcast Survival by Water Year for Winter-Run Chinook Salmon

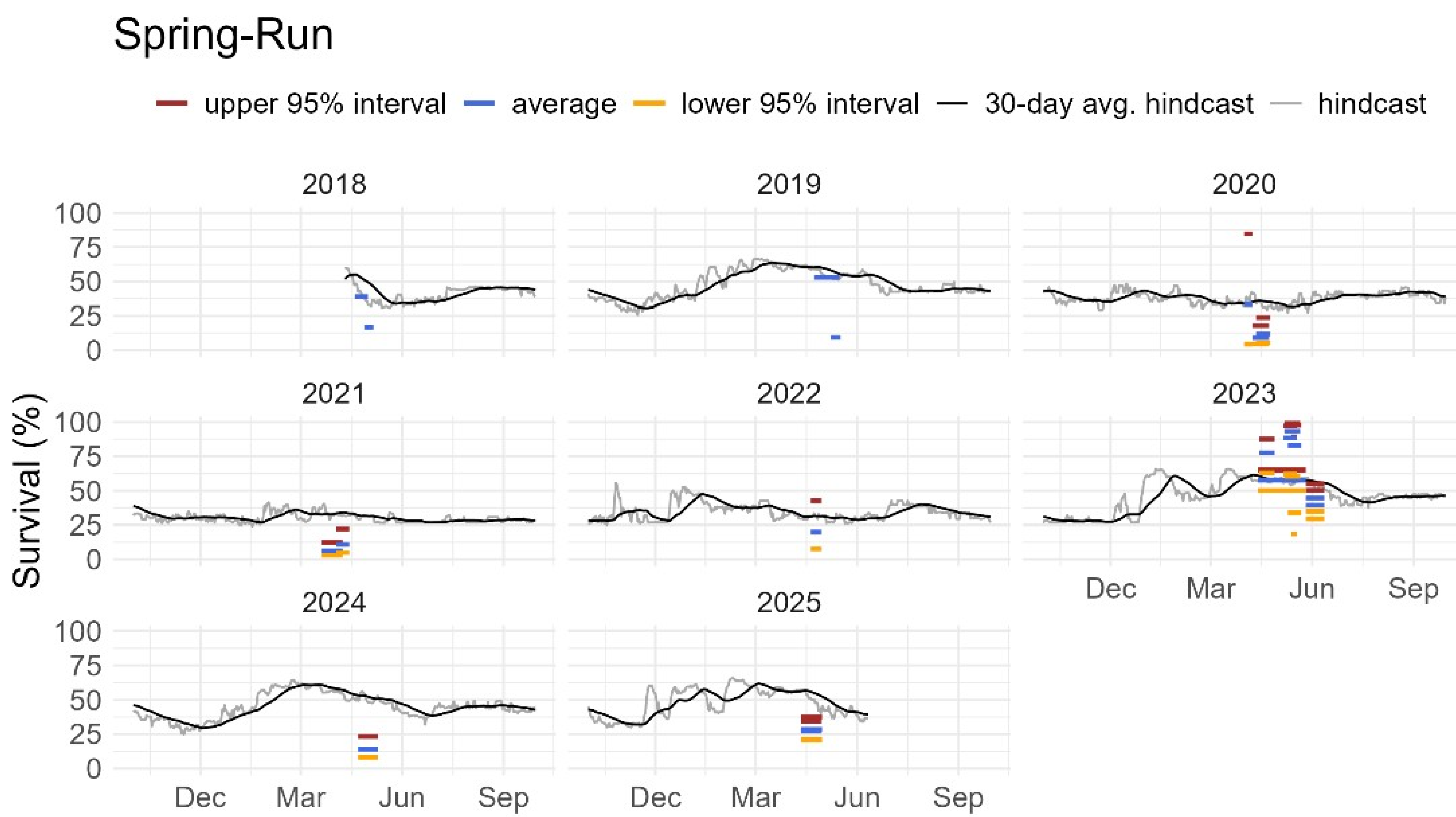

Note: Acoustic tag studies are shown as the average survival and 95% confidence interval for every study-release group combination and the ECO-PTM Emulator Hindcast Survival are shown as daily and 30-day running averages

Key: ECO-PTM = Ecological Particle Tracking Module

Figure 21. Comparison Between the Observed Survival from Acoustic Tag Studies and the ECO-PTM Emulator Hindcast Survival by Water Year for Spring-Run Chinook Salmon

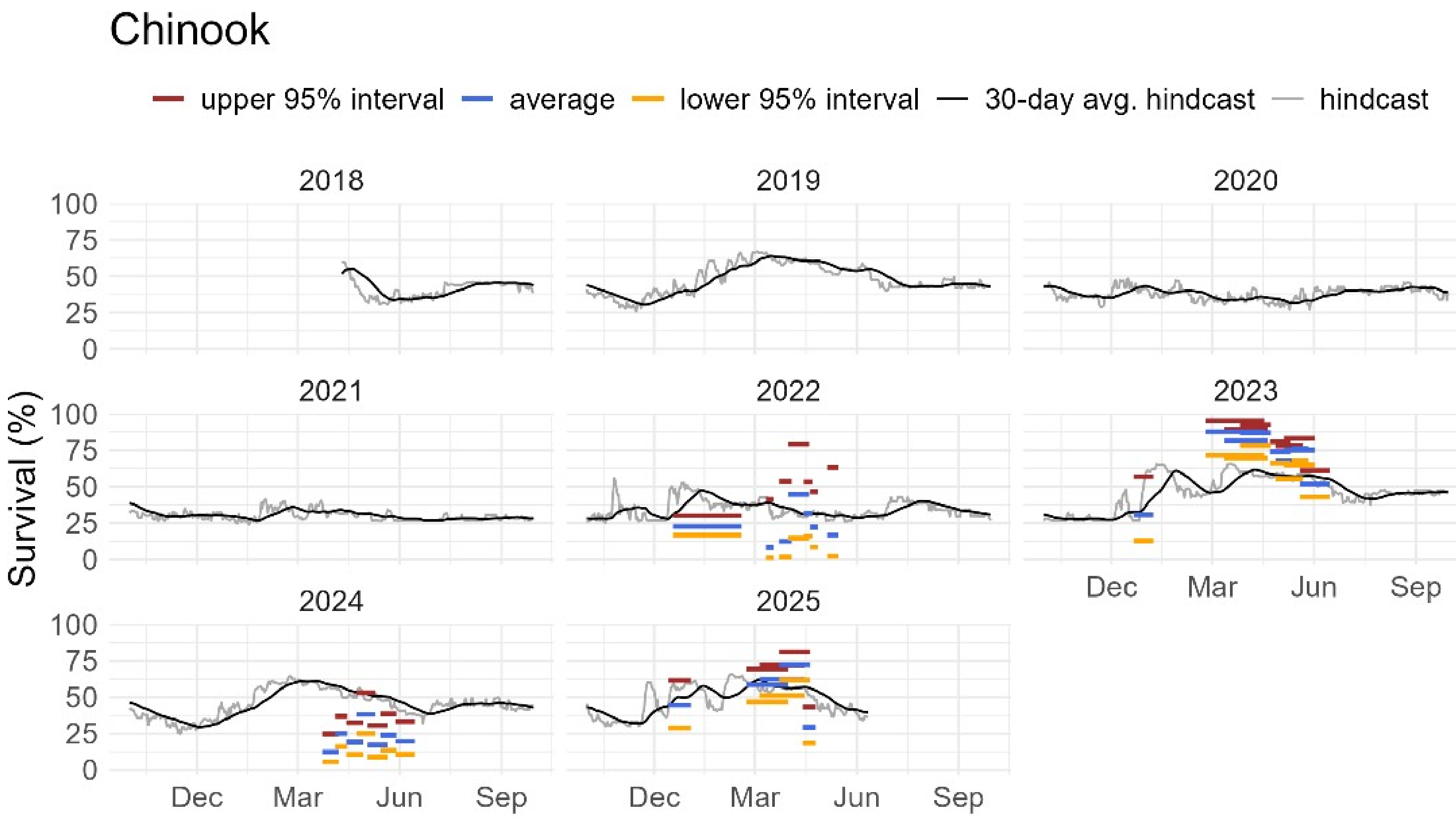

Note: Acoustic tag studies are shown as the average survival and 95% confidence interval for every study-release group combination and the ECO-PTM Emulator Hindcast Survival are shown as daily and 30-day running averages

Key: ECO-PTM = Ecological Particle Tracking Module

Figure 22. Comparison Between the Observed Survival from Acoustic Tag Studies and the ECO-PTM Emulator Hindcast Survival by Water Year for Studies that Included Unspecified or Mixed of Chinook Salmon

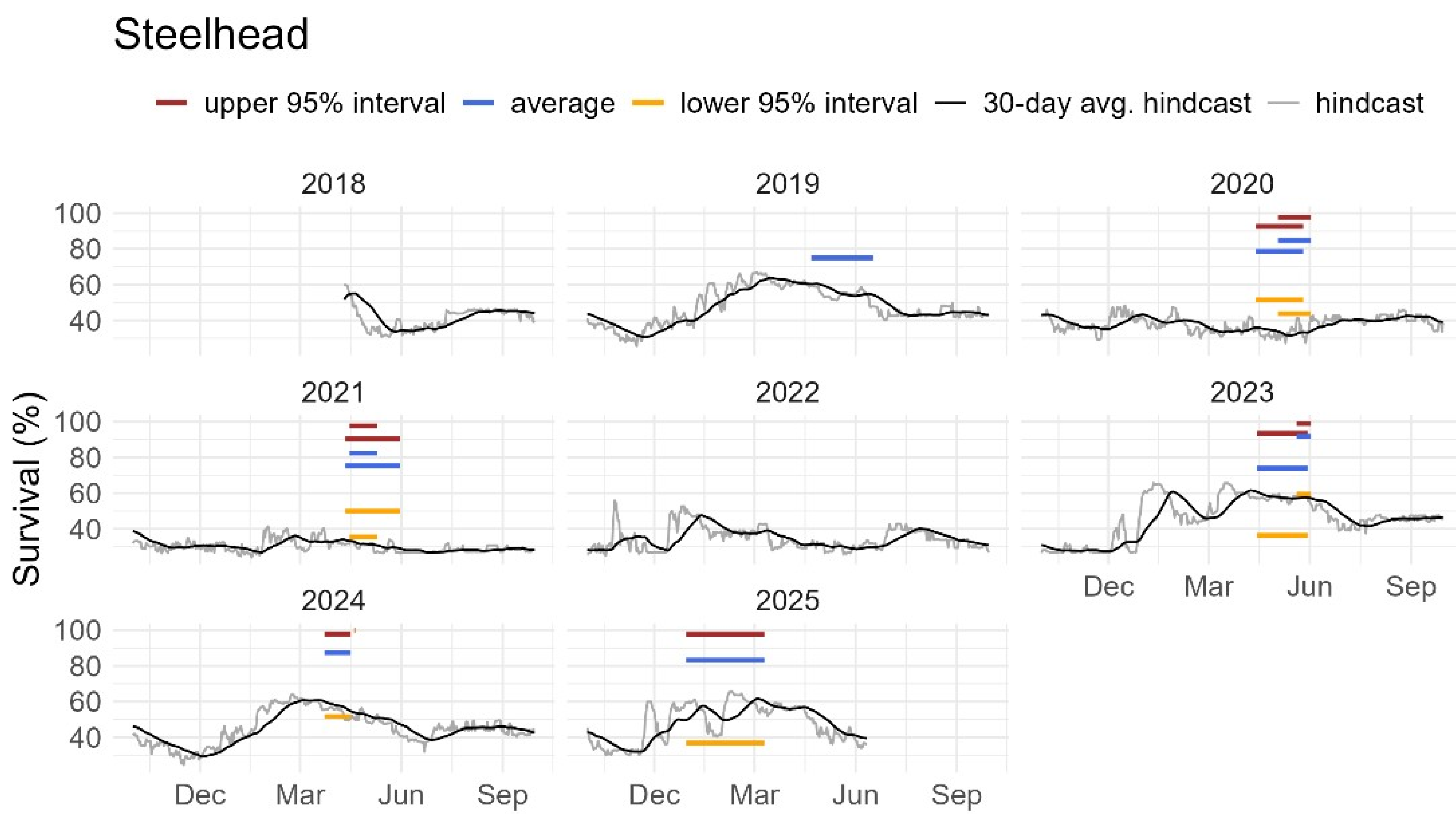

Note: Acoustic tag studies are shown as the average survival and 95% confidence interval for every study-release group combination and the ECO-PTM Emulator Hindcast Survival are shown as daily and 30-day running averages
Key: ECO-PTM = Ecological Particle Tracking Module

Figure 23. Comparison Between the Observed Survival from Acoustic Tag Studies and the ECO-PTM Emulator Hindcast Survival by Water Year for Steelhead

Hindcast Analysis: Entrainment at The Export Facilities

We compared the hindcast 50% entrainment event horizon against estimated historical entrainment (including expanded salvage and loss) of all Chinook Salmon runs and Steelhead. Our assumption about transport being a necessary but insufficient condition for entrainment was well supported for Late-Fall and Winter-Run Chinook Salmon as well as Steelhead, especially early in the season from December through March when they were relatively abundant (Figure 24, the first, fourth, and fifth rows). Seasonal patterns of the estimated historical entrainment of Winter-Run (Figure 25) and Steelhead (Figure 26) also trended well with the seasonal fluctuation of the entrainment event horizon. In most years, both Winter-Run and Steelhead had higher levels of entrainment early in the season corresponding to a high entrainment event horizon, and these values all decreased together later in the season. The low entrainment in high-risk scenarios seen in Figure 24 can be seen in the rising limbs of historical entrainment in Figure 25 and Figure 26, which again supports our assumption and could be attributed to fish distribution and the timing of their entry into the Delta. In addition to the typical seasonal trends, the entrainment event horizon also picked up the less common, delayed entrainment risk late in the season, where entrainment could increase again after the typical seasonal decrease if fish were still present. Examples include water year 1995, 2011, or 2017 (Figure 25 and Figure 26).

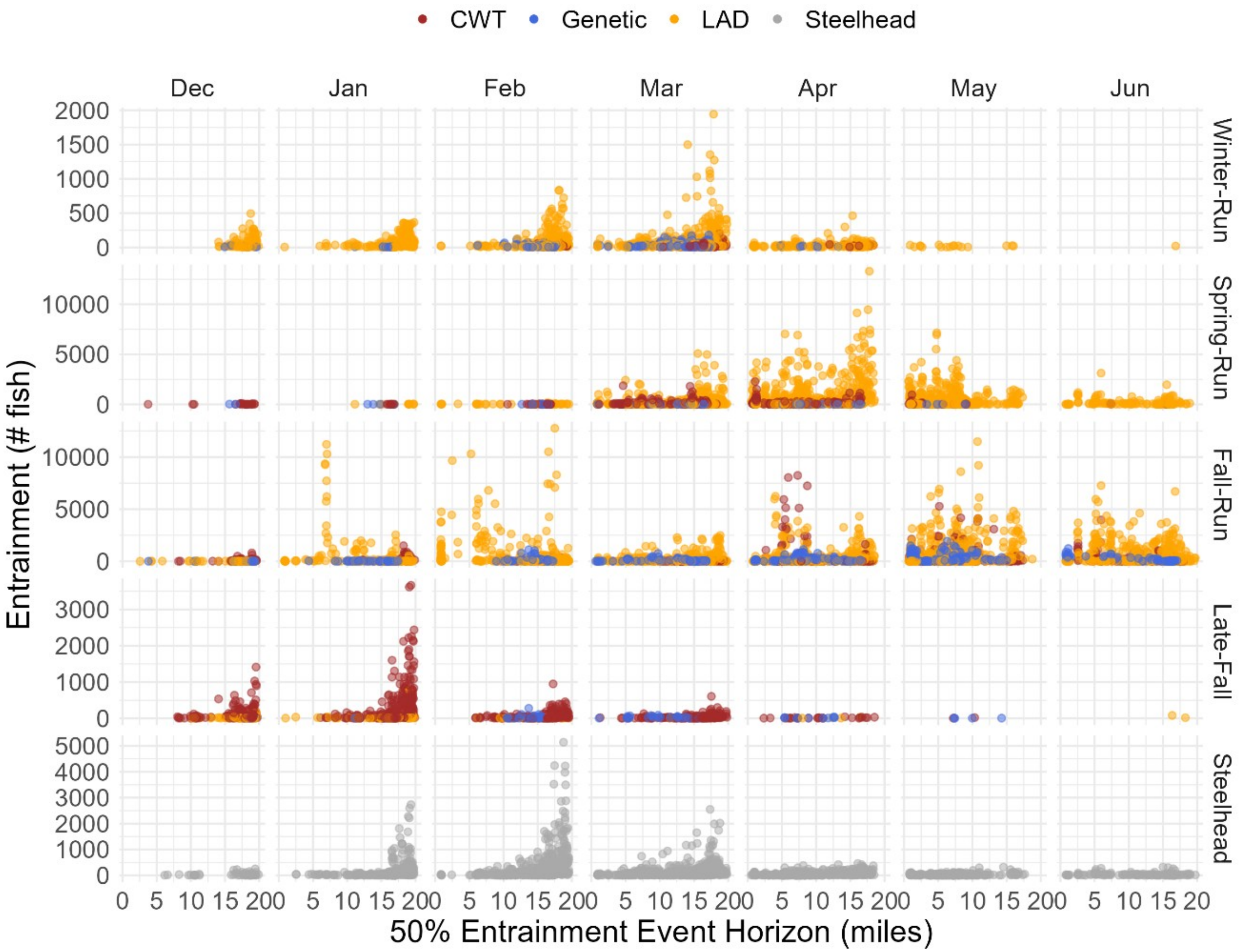

Note: Note that y axes are species-specific to account for population differences and for visibility. Figures are color-coded by Chinook salmon run identification methods including Coded Wire tag (CWT), Genetic Identification (Genetic), and Length-at-Date Estimation (LAD)

Figure 24 Scatter Plot of the 50% Entrainment Event Horizon Against the Estimated Historical Entrainment (i.e., salvage and plus loss), by Species (rows) and by Month (columns)

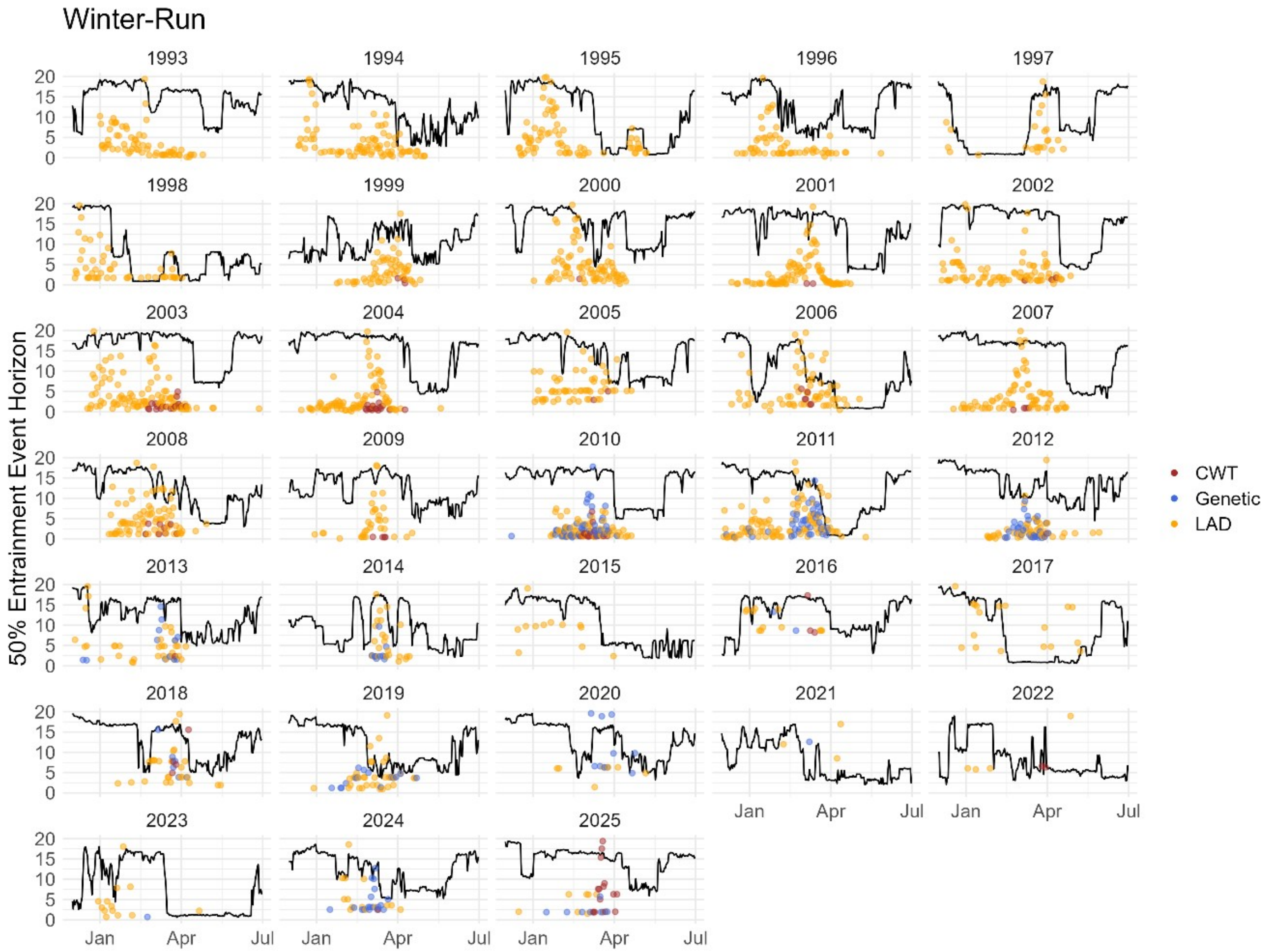

Note: The historical entrainment is rescaled to match the range of the entrainment event horizon in each water year for the purpose of showing the seasonal trend rather than the magnitude of entrainment. Figures are color-coded by identification method

Figure 25. Time Series Plots by Water Year of the Hindcast 50% Entrainment Event Horizon (black curve) and Winter-Run Estimated Historical Entrainment

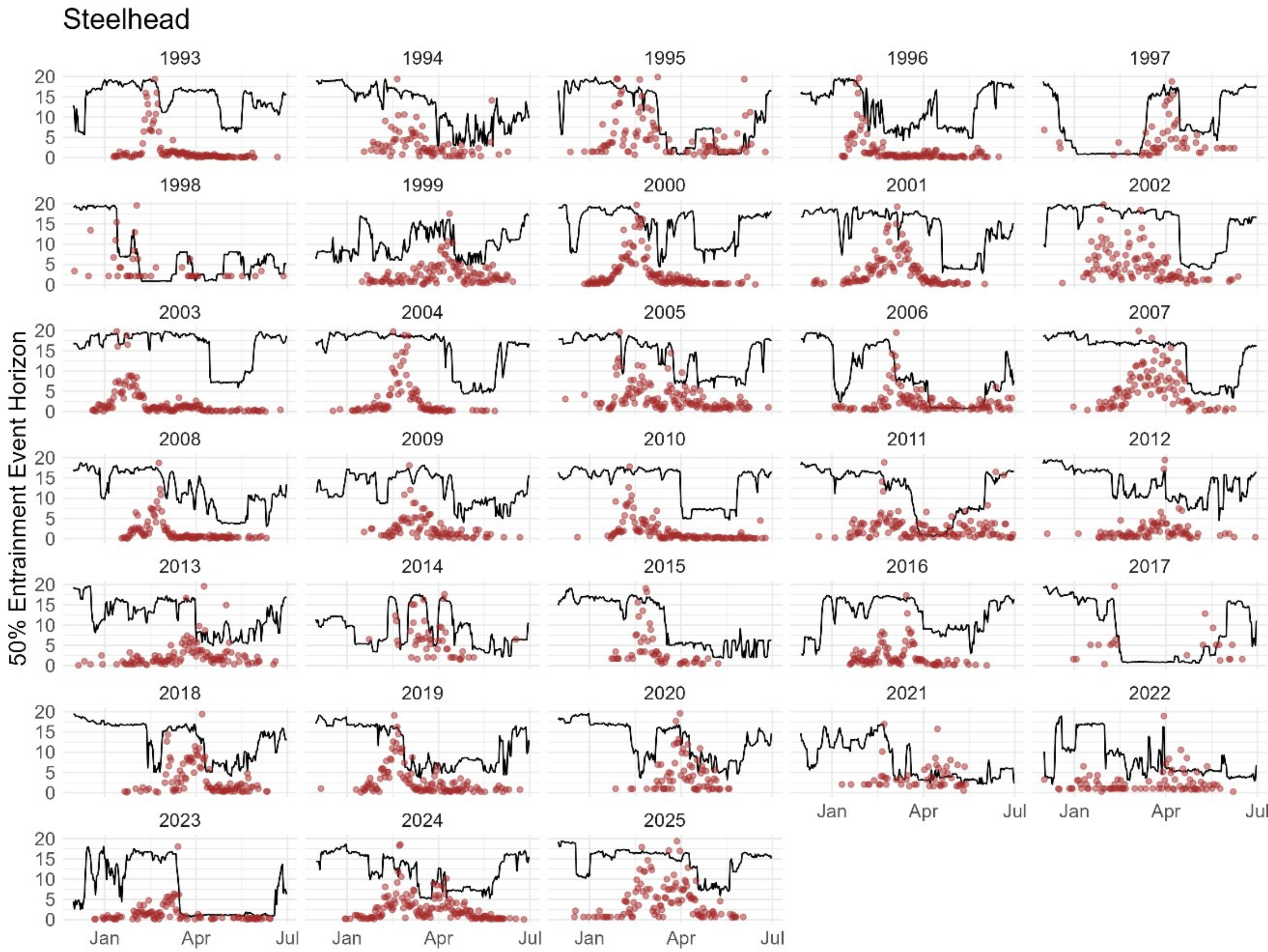

Note: The historical entrainment is rescaled to match the range of the entrainment event horizon in each water year for the purpose of showing the seasonal trend rather than the magnitude of entrainment.

Figure 26. Time Series Plots by Water Year of the Hindcast 50% Entrainment Event Horizon (black curve) and Steelhead Estimated Historical Entrainment

Unlike for the Winter-Run, Late-Fall Run, and Steelhead, we observed some unexpected high entrainment of Spring-Run and Fall-Run when the entrainment event horizon was low (Figure 24, second and third rows). This can also be observed in Figure 27 where in many years the trend of the entrainment event horizon is out of phase with that of Spring-Run entrainment, such as 2006. It is worth noting that most of the Spring-Run entrainment, especially in the early years studied, were identified by the length-at-date approach and thus many could be genetic Fall-Run misclassified as Spring-Run. While many of the length-at-date Spring-Run are likely unmarked hatchery genetic Fall-Run smolts, some may be Fall-Run outmigrants from the San Joaquin Basin, where smolts could be larger and mature earlier (Brandes et al. 2021; Satterthwaite et al. 2017). To that end, we further compared the estimated historical entrainment of Spring-Run with the hindcast 7-day particle entrainment of particles inserted at Vernalis using the PTM emulator (Figure 28). This comparison provides a different set of insights because the entrainment event horizon was designed to best reflect the entrainment risk in central and south Delta along the Old and Middle River corridors, but may not fully reflect the entrainment risk for fish entering the Delta from the San Joaquin River basin. As shown in Figure 28, Spring-Run entrainment trended well with the entrainment risk from Vernalis, but that correlation had subtle changes across different levels of entrainment event horizon, indicating the interplay between export, San Joaquin Delta inflow, and the hydrodynamics in central and south Delta. Another insight we gained from this comparison is the importance of spatial heterogeneity in entrainment risk, and that the proposed tools, including the hydraulic footprints and the emulators, are best to be used together to obtain a comprehensive understanding of entrainment.

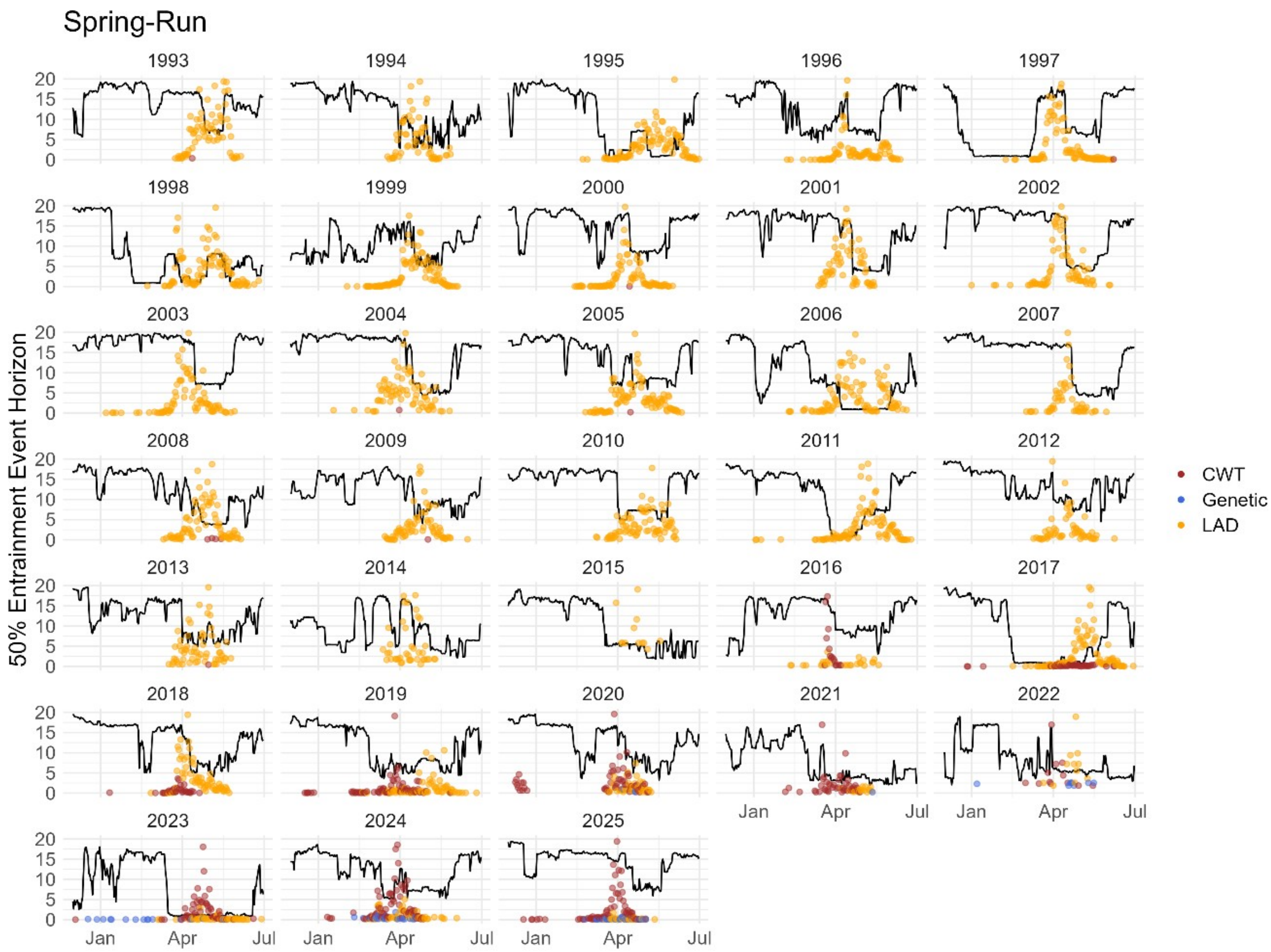

Note: The historical entrainment is rescaled to match the range of the entrainment event horizon in each water year for the purpose of showing the seasonal trend rather than the magnitude of entrainment. Figures are color-coded by identification method

Figure 27. Time Series Plots by Water Year of the Hindcast 50% Entrainment Event Horizon (black curve) and Spring-Run Estimated Historical Entrainment

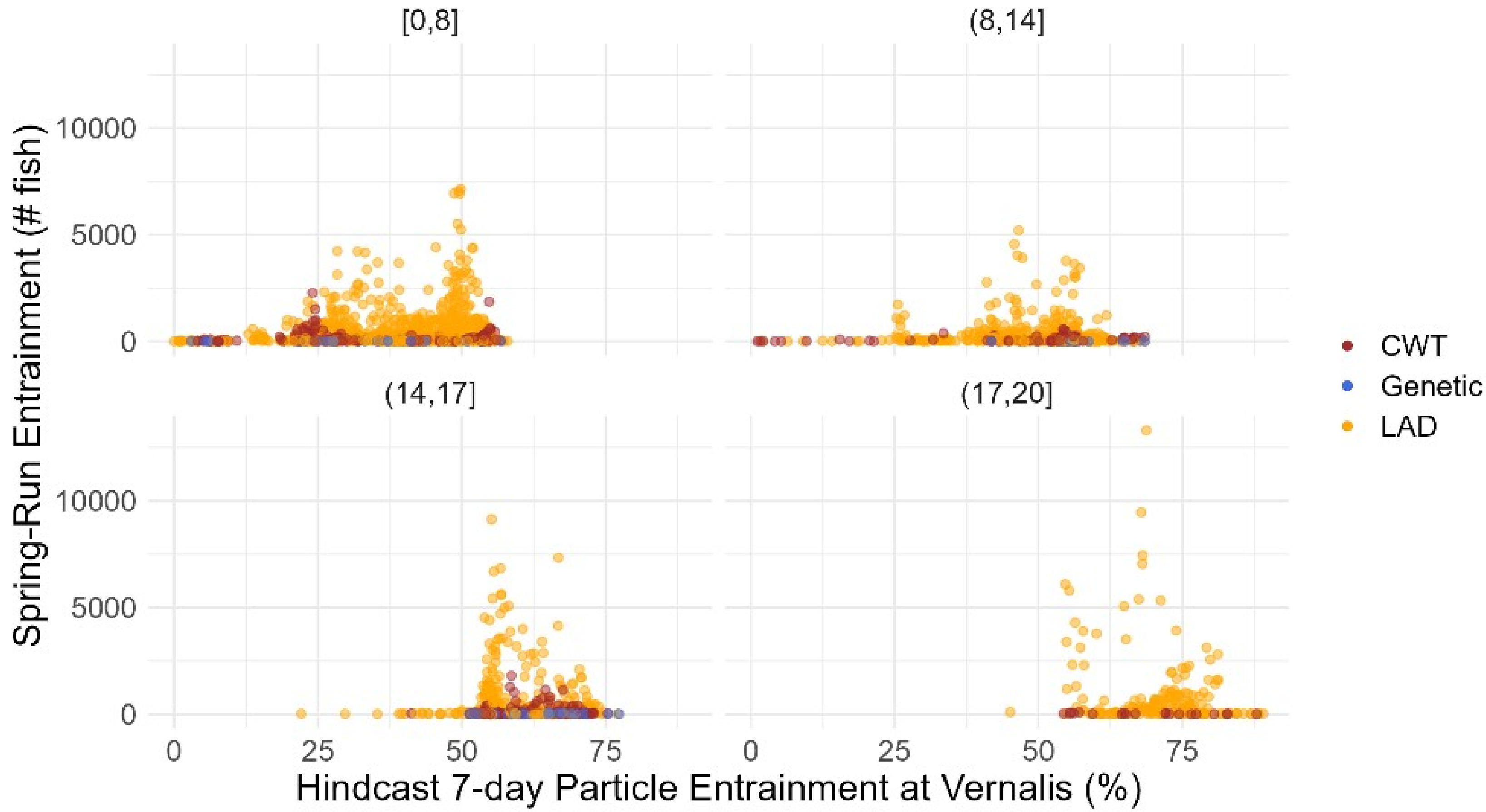

Note: Color-coded by identification method and grouped by quartiles of the 50% entrainment event horizon (e.g., "(8,14)" means larger than 8 and lower than or equal to 14 miles).

Figure 28. Scatter Plots of the Hindcast 7-Day Particle Entrainment of Particles Inserted at Vernalis from the PTM Emulator Against the Historical Spring-Run Entrainment

Inverse Modeling Analysis

To demonstrate the applicability of the tools proposed herein, we chose the period between January and February in 2019 to conduct an inverse modeling analysis. Over this period, CVP and SWP exports were managed to maintain a fixed level of OMR at -5,000 cfs to limit species entrainment. We used the predictive model to hindcast the 15% entrainment event horizon value on January 4th and February 4th, and also estimated the values under a range of hypothetical export scenarios from 1,500 cfs to 10,000 cfs at 100-cfs intervals while keeping all other conditions the same as historical conditions (Figure 29). The hindcast entrainment event horizon ranged from the south of Franks Tract (i.e., still within the Old and Middle River corridor) to beyond Franks Tract. Under the context of adaptive management, one could take into account the distribution of species or environmental factors at the time to determine the relevance of risk management with regard to Franks Tract. For example, if targeted species were found in surveys in Franks Tract, given the flow conditions of January 4th, 2019 export could be reduced to around 3,000 cfs to limit the high-risk zone to the south of Franks Tract. In contrast, if targeted species were found mostly downstream near the confluence of Sacramento and San Joaquin Rivers, given the flow conditions on February 4th, 2019 perhaps export could be increased to near capacity without extending the high-risk zone further beyond Franks Tract.

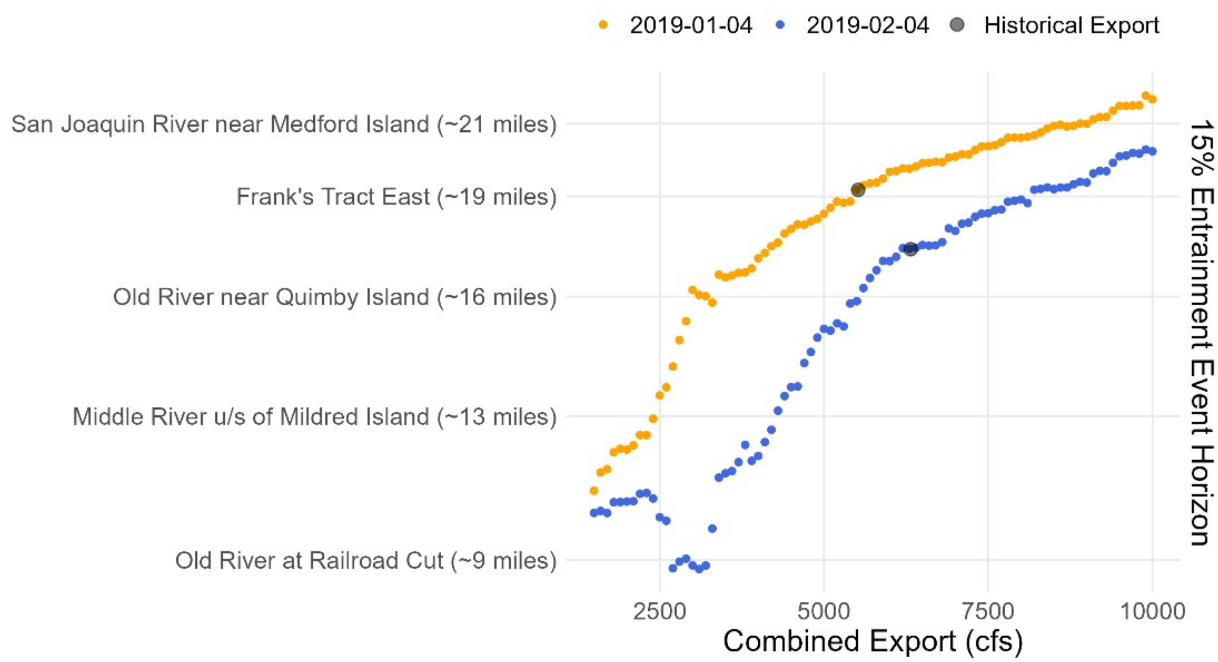

Note: Key locations and their distances from Clifton Court Forebay gates are annotated for referencing the location of the entrainment event horizon.

Figure 29. Inverse Modeling Analysis of the 15% Entrainment Event Horizon with Historical Conditions on January 4th and February 4th, 2026

We further visualized the inverse modeling results by showing the spatial distribution of entrainment risk at different hypothetical export levels under the flow conditions of February 4th, 2019 (Figure 30). At the minimum level of export (1,500 cfs, corresponding to historical public health and safety levels), entrainment risk was confined to the close vicinity of the export facilities, as expected. At a moderate level closer to historical export, high entrainment risk extended throughout the Old and Middle River corridors but not into Franks Tract, while the risk at upstream San Joaquin River were elevated but not as high and did not carry downstream. At a high export level near 9,000 cfs, entrainment risks in Franks Tract and downstream Old and Middle River corridor further elevated, and minor risks along San Joaquin River started to manifest, but the risks at upstream San Joaquin River remained the same. This is yet another example of how the hydraulic footprints and the emulators can be used together to reveal spatial insights. For example, one might factor in the design of alternative operations whether the species of interest at the time mainly originated from the San Joaquin Basin, and evaluate the efficacy of restricting exports to various levels.

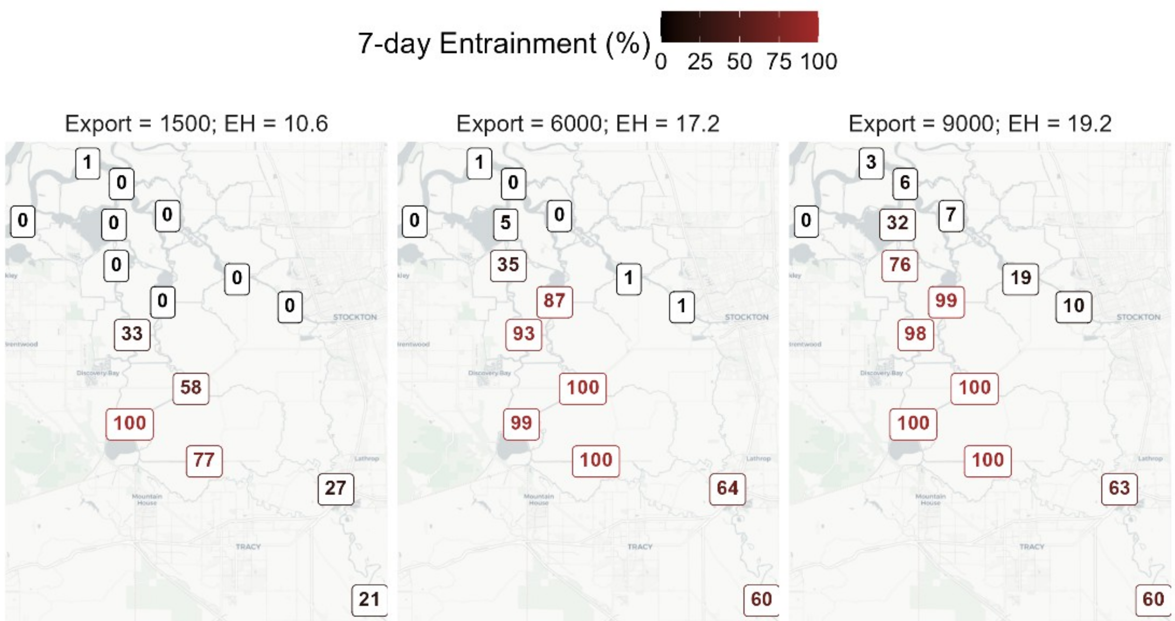

Note: The particle entrainment level is both color-coded and annotated.
Key: cfs = cubic feet per second
PTM = Particle Tracking Module

Figure 30. Spatial Distribution Across Central and South Delta of the Estimated 7-day Particle Entrainment from the PTM Emulator Under Three Different Export Levels (1,500, 6,000, and 9,000 cfs) Given the Flow Conditions of February 4th, 2019, with the Corresponding Entrainment Event Horizon (EH, miles)

Although the target entrainment threshold, export levels, and historical flow conditions were arbitrarily chosen for illustration purposes, the conclusion from the inverse analysis is general and applicable in practice. The critical innovations are that alternative export operations can be, and ideally should be, designed around risks rather than average flows, and that one can design such alternative operations using our tools with simpler (compared to running a hydrodynamic model) and readily available input data. Assessing the marginal impact of changes in operations can be done in seconds, which is valuable for real-time operations management or large-scale analyses involving thousands of detailed, nuanced alternatives.

5. Discussion

Model Limitations

The tools proposed herein were based on the OMR Sensitivity Study with outputs from CalSim and DSM2 modeling treated as simulated data (Section 3.1). Therefore, limitations on our proposed tools arise from both the model simulations in the OMR Sensitivity Study as well as the study itself.

To begin with, DSM2 ECO-PTM uses several models from prior studies to calculate routing and survival, such as the exposure-time survival model with region-specific parameters (Anderson et al. 2005; Wang et al. 2024) and the statistical models for routing at key junctions (D. Hance et al. 2020; Perry et al. 2015; Romine et al. 2020). ECO-PTM was calibrated on juvenile Late-Fall-Run Chinook Salmon outmigration data from the Sacramento basin, and currently does not have the capability of modeling San Joaquin-origin salmonids. Being an emulator, the ECO-PTM emulator naturally carries these limitations forward and thus is applicable only when ECO-PTM is.

Similarly, the PTM emulator and the hydraulic footprints carry forward the limitations in DSM2 PTM, such as the lack of biological or ecological effects (e.g., individual swimming behavior, or predation during transport, etc.). In addition, some limitations on DSM2 HYDRO may affect the calculation of transport in central and south Delta, including the approximation of Franks Tract as an instantly well-mixed reservoir, outdated channel connectivity and bathymetry in the south Delta, and outdated boundary conditions for Delta consumptive uses. While DWR has invested efforts to update the channel grids and boundary conditions, those recent updates were not reflected in the simulated data.

Some additional limitations arise from the range of conditions included in the OMR Sensitivity Study. Although a wide range hypothetical export management strategies were modeled, and the resulting CVP and SWP exports spanned a much wider range than the historical records in recent years, the combinations of Delta inflows and exports were still largely within the scope of recent regulations due to other regulatory components beyond the Old and Middle River corridor (e.g., Delta outflow management). To that end, application of the emulators and hydraulic footprints in extreme cases (e.g., near-capacity combined export during droughts) is not advised, where a full hydrodynamic model simulation may be more useful.

Bridging the Gap between Hydrodynamics and Species Responses

In this study we proposed the hydraulic footprints as standalone tools, and we demonstrated their accuracy and applicability with spatial patterns, cross-validation, hindcast analyses, and inverse analyses, but we also acknowledged that they are hydrodynamic-based tools and thus do not account for biological, ecological, and environmental factors. However, the hydraulic footprints do not have to be applied in isolation. We purposefully developed them to be intuitive and amiable to a non-technical audience, to make it easy for integration into a larger study scope.

Prior studies have been evaluating the impact of exports on targeted species via exports itself, Vernalis flow, OMR flow, or some export-based metrics such as the export-inflow ratio (Grimaldo et al. 2009, 2021; Hamilton et al. 2025; Smith et al. 2021; Tillotson et al. 2022). These flow-based metrics may contain partial information on transport but do not account for tidal dispersive transport. Although we did not conduct a full comparative analysis on metrics versus the hydraulic footprint, a simple exploratory comparison is enough to show how important it is to account for hydrodynamics in species entrainment (Figure 31), which shows that moderate level of entrainment could occur under less negative or even positive OMR, but never under low entrainment event horizon.

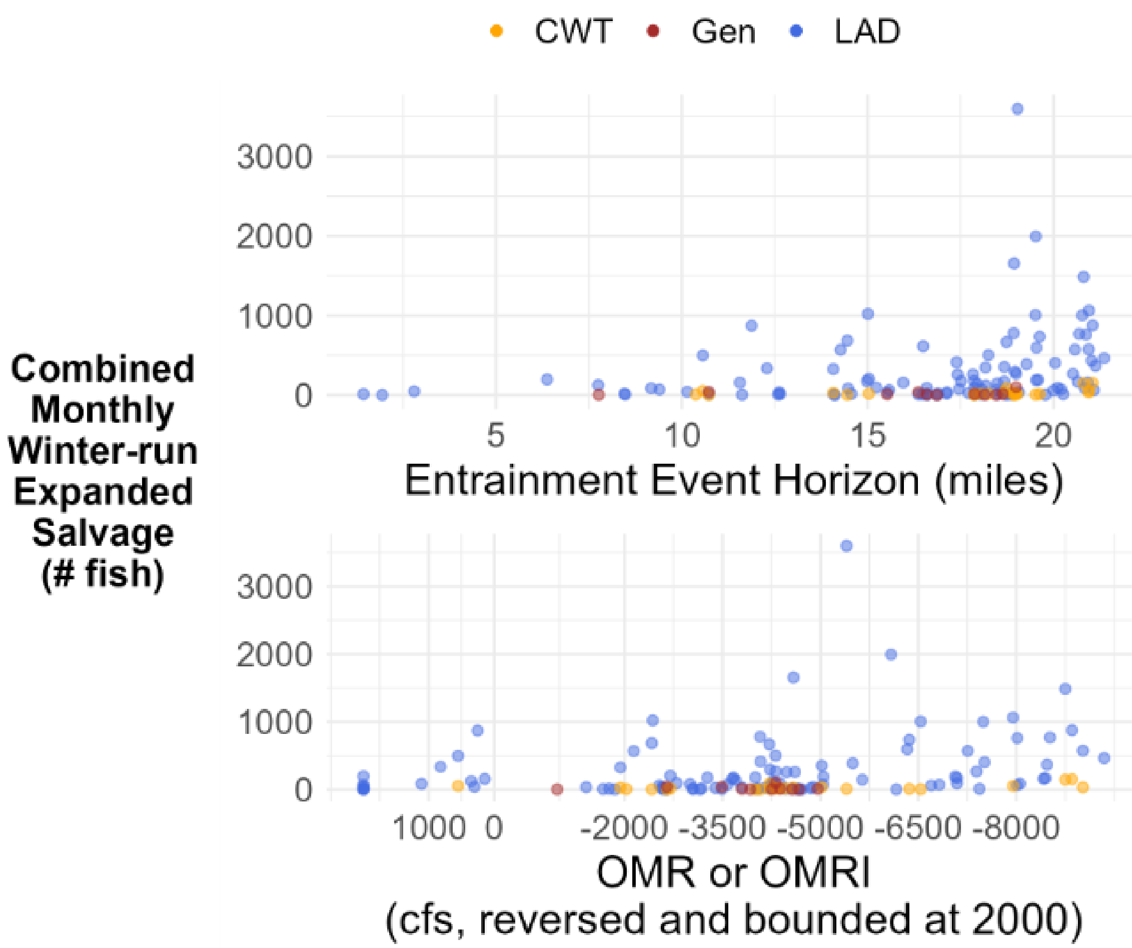

Note: Color-coded by identification method where "CWT" means coded wire tag, "Gen" means genetically identified, and "LAD" means length-at-date estimation.

Key:
CVP = Central Valley Project
OMR = Old and Middle River
OMRI = Old and Middle River Index
SWP = State Water Project

Figure 31. Scatter Plots of the Monthly Average Hindcast 15% Entrainment Event Horizon (top) and the Monthly Average OMR (or OMRI when OMR data were missing, bottom) Versus the Combined CVP and SWP Monthly Expanded Salvage of Winter-run Chinook Salmon

We hereby offer the hydraulic footprints as metrics that can be used as inputs to other species analyses. These analyses could be as complicated as salmonid or smelt life-cycle models, or as simple as a direct comparison between species observations and the hydraulic footprints, or anywhere in between. An example is the hindcast analysis presented in this study, where we compared the hindcast entrainment event horizon and entrainment values with the estimated historical entrainment. The effects of exports on salmonid entrainment have been hypothesized in various ways: whether reduced export encourages volitional swimming and outmigration, or whether reduced exports increase travel time and in turn increase predation mortality. The results of our hindcast analysis supported the conceptual assumption that transport is a necessary but insufficient condition for predicting entrainment, and further highlighted the differences in risk for Sacramento-origin fish versus San Joaquin-origin fish. While these findings do not directly prove or disprove the aforementioned hypotheses, the hindcast analysis can be further improved in future studies by a more rigorous consideration of salmonid behaviors and responses to advance our understandings on the issue.

6. Conclusion

In this study, we developed emulator models to estimate entrainment and salmonid responses in the Delta while bypassing the technical efforts of running hydrodynamic models. Furthermore, we developed hydraulic footprints, which are intuitive and quantitative metrics that account for the underlying transport processes and summarize the spatial context in entrainment risk into a simple form. The hydraulic footprints can be predicted with high accuracy while requiring only simple and readily available input data, making them suitable for real-time adaptive management or large-scale analyses involving hundreds of alternatives. We conducted hindcast and inverse analyses to demonstrate how the hydraulic footprints can be used to directly quantify the marginal effects of alternative operations, how they matched well with historical observations, and how they represent a pivotal advance in the science on protected species in the Delta by providing an improved representation of hydrodynamics. The tools proposed herein are intended to be responsive to the recommendations from the NAS and DSP independent reviews on LTO and the current management tools, by offering a mechanistic, proactive, and spatially explicit approach for operations management.

7. References

Anderson, J.J., E. Gurarie, and R.W. Zabel. 2005. Mean free-path length theory of predator–prey interactions: Application to juvenile salmon migration. Ecological Modelling, 186(2), 196–211. https://doi.org/10.1016/j.ecolmodel.2005.01.014

Brandes, P.L., B. Pyper, M. Banks, D. Jacobson, T. Garrison, and S. Cramer. 2021. Comparison of Length-at-Date Criteria and Genetic Run Assignments for Juvenile Chinook Salmon Caught at Sacramento and Chipps Island in the Sacramento–San Joaquin Delta of California. San Francisco Estuary and Watershed Science, 19(3). https://doi.org/10.15447/sfews.2021v19iss3art2

Buchanan, R.A., and J. Ferguson. 2017a. CSAMP Salmon Scoping Team Report. Volume 1.

Buchanan, R.A., and J. Ferguson. 2017b. CSAMP Salmon Scoping Team Report. Volume 2: Responses to Management Questions.

U.S. Bureau of Reclamation (Reclamation). 2025a. Attachment I.2: Salvage Density Model Loss

California Department of Fish and Wildlife. 2018. Chinook Salmon Loss Estimation for Skinner Delta Fish Protective Facility and Tracy Fish Collection Facility. https://filelib.wildlife.ca.gov/Public/salvage/Salmon%20loss%20estimation.docx

California Department of Fish and Wildlife. 2024. Incidental Take Permit for Long-Term Operations of the State Water Project. California Department of Fish and Wildlife. November 5, 2024. https://www.acwa.com/news/new-incidental-take-permit-issued-for-state-water-project/}

California Department of Water Resources. No Date. Dayflow: An estimate of daily average Delta outflow (Version 2025) [Dataset]. Retrieved March 4, 2026, from https://water.ca.gov/Programs/Environmental-Services/Compliance-Monitoring-And-Assessment/Dayflow-Data. As of May 4, 2036, data available from: https://data.cnra.ca.gov/dataset/dayflow

California Department of Water Resources. 2023. State Water Project Final Delivery Capability Report. State of California, Natural Resources Agency.

Cavallo, B., P. Bergman, and J. Melgo. 2011. The Delta Passage Model. Cramer Fish Sciences. https://www.researchgate.net/profile/Bradley-Cavallo-2/publication/268203895_The_Delta_Passage_Model/links/5810f9bd08aea04bbcbd4c41/The-Delta-Passage-Model.pdf

Draper, A.J., A. Munévar, S.K. Arora, E. Reyes, N.L. Parker, F.I. Chung, and L.E. Peterson. 2004. CalSim: Generalized model for reservoir system analysis. Journal of Water Resources Planning and Management, 130(6), 480–489.

Ferguson, J., and B. Cavallo. 2024. A Review of Recent Science to Improve Understanding and the Application of Life Cycle and Decision Support Models to Salmon Management in the South Delta. CSAMP Salmon Technical Working Group.

Fleenor, W.E., and F. Bombardelli. 2013. Simplified 1-D Hydrodynamic and Salinity Transport Modeling of the Sacramento–San Joaquin Delta: Sea Level Rise and Water Diversion Effects. San Francisco Estuary and Watershed Science, 11(4). https://doi.org/10.15447/sfews.2013v11iss4art2

Godichon-Baggioni, A., C. Maugis-Rabusseau, and A. Rau. 2020. Multiview cluster aggregation and splitting, with an application to multiomic breast cancer data. The Annals of Applied Statistics, 14(2). https://doi.org/10.1214/19-aoas1317

Grimaldo, L., M. Nobriga, and W. Smith. 2020. Adult Delta Smelt Entrainment, Study 1—Factors Associated with Salvage (p. 156). Collaborative Science and Adaptive Management Program.

Grimaldo, L., W. Smith, and M. Nobriga. 2021. Re-Examining Factors That Affect Delta Smelt (*Hypomesus transpacificus*) Entrainment at the State Water Project and Central Valley Project in the Sacramento–San Joaquin Delta. San Francisco Estuary and Watershed Science, 19(1). https://doi.org/10.15447/sfews.2021v19iss1art5

Grimaldo, L., T. Sommer, Nick Van Ark, G. Jones, E. Holland, P.B. Moyle, B. Herbold, and P. Smith. 2009. Factors Affecting Fish Entrainment into Massive Water Diversions in a Tidal Freshwater Estuary: Can Fish Losses be Managed? North American Journal of Fisheries Management, 29(5), 1253–1270. https://doi.org/10.1577/m08-062.1

Gross, E., S. Andrews, B. Bergamaschi, B. Downing, R. Holleman, S. Burdick, and J. Durand. 2019. The Use of Stable Isotope-Based Water Age to Evaluate a Hydrodynamic Model. Water, 11(11), 2207. https://doi.org/10.3390/w11112207

Gross, E., W. Kimmerer, J. Korman, L. Lewis, S. Burdick, and L. Grimaldo. 2022. Hatching distribution, abundance, and losses to freshwater diversions of longfin smelt inferred using hydrodynamic and particle-tracking models. Marine Ecology Progress Series, 700, 179–196. https://doi.org/10.3354/meps14168

Hamilton, S.A., D.D. Murphy, and E.L. Montoya. 2025. Identifying the environmental conditions that determine the distribution of an endangered estuarine fish to manage risk of entrainment. Frontiers in Ecology and Evolution, 13. https://doi.org/10.3389/fevo.2025.1411994

Hance, D.J., R.W. Perry, A.C. Pope, A.J. Ammann, J.L. Hassrick, and G. Hansen. 2022. From drought to deluge: Spatiotemporal variation in migration routing, survival, travel time and floodplain use of an endangered migratory fish. Canadian Journal of Fisheries and Aquatic Sciences, 79(3), 410–428. https://doi.org/10.1139/cjfas-2021-0042

Hance, D., R. Perry, J. Burau, A. Blake, P. Stumpner, X. Wang, and A. Pope. 2020. Combining Models of the Critical Streakline and the Cross-Sectional Distribution of Juvenile Salmon to Predict Fish Routing at River Junctions. San Francisco Estuary and Watershed Science, 18(1). https://doi.org/10.15447/sfews.2020v18iss1art3

Hutton, P. 2008. A model to estimate combined Old and Middle River Flows. Metropolitan Water District of Southern California.

Interagency Ecological Program. 2015. An updated conceptual model of Delta Smelt biology: Our evolving understanding of an estuarine fish (Technical Report 90). Interagency Ecological Program for the San Francisco Bay/Delta Estuary.

John, C.R., D. Watson, M.R. Barnes, C. Pitzalis, and M.J. Lewis. 2019. Spectrum: Fast density-aware spectral clustering for single and multi-omic data. Bioinformatics, 36(4), 1159–1166. https://doi.org/10.1093/bioinformatics/btz704

Kimmerer, W.J. 2008. Losses of Sacramento River Chinook Salmon and Delta Smelt to Entrainment in Water Diversions in the Sacramento–San Joaquin Delta. San Francisco Estuary and Watershed Science, 6(2). https://doi.org/10.15447/sfews.2008v6iss2art2

MacWilliams, M., A.J. Bever, E.S. Gross, G.S. Ketefian, and W.J. Kimmerer. 2015. Three-Dimensional Modeling of Hydrodynamics and Salinity in the San Francisco Estuary: An Evaluation of Model Accuracy, X2, and the Low-Salinity Zone. San Francisco Estuary and Watershed Science, 13(1). https://doi.org/10.15447/sfews.2015v13iss1art2

National Academies of Sciences, Engineering and Medicine. 2025. Review of the Long-Term Operations of the Central Valley Project and the State Water Project. The National Academies Press. https://doi.org/10.17226/29130

National Marine Fisheries Service. 2009. Biological Opinion on Long-Term Operations of the Central Valley Project and State Water Project. National Marine Fisheries Service Southwest Region.

National Marine Fisheries Service. 2024. Endangered Species Act Section 7(a)(2) Programmatic Biological Opinion for the Reinitiation of Consultation on the Long-Term Operation of the Central Valley Project and State Water Project. National Oceanic and Atmospheric Administration, West Coast Region. December 6, 2024. https://www.fisheries.noaa.gov/resource/document/endangered-species-act-section-7a2-programmatic-biological-opinion-reinitiation

National Oceanic and Atmospheric Administration. No Date. CalFishTrack: Central Valley Enhanced Acoustic Tagging Project [Dataset]. Retrieved March 31, 2026, from https://oceanview.pfeg.noaa.gov/CalFishTrack/index.html

Newman, K.B. 2003. Modelling paired release–recovery data in the presence of survival and capture heterogeneity with application to marked juvenile salmon. Statistical Modelling, 3, 157–177.

Newman, K.B. 2008. An evaluation of four Sacramento–San Joaquin River Delta juvenile salmon survival studies. Report for Stockton Fish and Wildlife Office, U.S. Fish and Wildlife Service. March 31, 2008. 182 pages.

Newman, K.B., and P.L. Brandes. 2010. Hierarchical Modeling of Juvenile Chinook Salmon Survival as a Function of Sacramento–San Joaquin Delta Water Exports. North American Journal of Fisheries Management, 30, 157–169.

Newman, K.B., and J. Rice. 2002. Modeling the Survival of Chinook Salmon Smolts Outmigrating Through the Lower Sacramento River System. Journal of the American Statistical Association, 97, 983–993.

Perry, R.W., P.L. Brandes, J.R. Burau, P.T. Sandstrom, and J.R. Skalski. 2015. Effect of Tides, River Flow, and Gate Operations on Entrainment of Juvenile Salmon into the Interior Sacramento–San Joaquin River Delta. Transactions of the American Fisheries Society, 144(3), 445–455. https://doi.org/10.1080/00028487.2014.1001038

Perry, R.W., A.C. Pope, J.G. Romine, P.L. Brandes, J.R. Burau, A.R. Blake, A.J. Ammann, and C.J. Michel. 2018. Flow-mediated effects on travel time, routing, and survival of juvenile Chinook salmon in a spatially complex, tidally forced river delta. Canadian Journal of Fisheries and Aquatic Sciences, 75(11), 1886–1901. https://doi.org/10.1139/cjfas-2017-0310

Romine, J., R. Perry, P. Stumpner, A. Blake, and J. Burau. 2020. Effects of Tidally Varying River Flow on Entrainment of Juvenile Salmon into Sutter and Steamboat Sloughs. San Francisco Estuary and Watershed Science, 19(2). https://doi.org/10.15447/sfews.2021v19iss2art4

Satterthwaite, W.H., S.M. Carlson, and A. Criss. (2017). Ocean Size and Corresponding Life History Diversity among the Four Run Timings of California Central Valley Chinook Salmon. https://dx.doi.org/10.1080/00028487.2017.1293562

Smith, W.E., L. Polansky and M.L. Nobriga. 2021. Disentangling risks to an endangered fish: Using a state-space life cycle model to separate natural mortality from anthropogenic losses. Canadian Journal of Fisheries and Aquatic Sciences, 78(8), 1008–1029. https://doi.org/10.1139/cjfas-2020-0251

Sridharan, V.K., S.G. Monismith, O.B. Fringer, and D.A. Fong. 2018. Evaluation of the Delta Simulation Model-2 in Computing Tidally Driven Flows in the Sacramento-San Joaquin Delta. San Francisco Estuary and Watershed Science, 16(2). https://escholarship.org/uc/item/0vm955tw

Sturrock, A.M., N.E. Monsen, and R.W. Zabel. 2026. Water Year 2024 and 2025 Winter-run Chinook Salmon Annual Loss Independent Peer Review. Delta Science Program, Delta Stewardship Council. https://deltacouncil.ca.gov/delta-science-program/water-year-2024-and-2025-winter-run-chinook-salmon-annual-loss-independent-peer-review

Tillotson, M., and J. Brandon. 2023. Evaluating the Influence of Proportional Entrainment Loss on Subadult Delta Smelt Survival Using the Maunder and Deriso in R (MDR) Model. ICF. https://csamp.baydeltalive.com/assets/eec462358f80cc8d9910bfda974fa6f4/application/pdf/REPORT_Evaluation_of_PEL_using_the_MDR.pdf

Tillotson, M., J. Hassrick, A. Collins, and C. Phillis. 2022. Machine Learning Forecasts to Reduce Risk of Entrainment Loss of Endangered Salmonids at Large-Scale Water Diversions in the Sacramento–San Joaquin Delta, California. San Francisco Estuary and Watershed Science, 20(2). https://doi.org/10.15447/sfews.2022v20iss2art3

University of Washington. No Date. SacPAS: Central Valley Prediction and Assessment of Salmon and other fishes [Dataset]. Retrieved April 7, 2026, from https://www.cbr.washington.edu/sacramento/

U.S. Bureau of Reclamation (Reclamation). 2025a. Attachment I.2: Salvage Density Model Loss Simulation. Long-Term Operations of the CVP and SWP. Available at: https://www.usbr.gov/mp/nepa/nepa_project_details.php?Project_ID=54661

U.S. Bureau of Reclamation (Reclamation). 2025b. Attachment I.3: Delta Export Zone of Influence Analysis. Long-Term Operations of the CVP and SWP. Available at: https://www.usbr.gov/mp/nepa/nepa_project_details.php?Project_ID=54661

U.S. Bureau of Reclamation (Reclamation). 2025c. Sensitivity Analysis of Old and Middle River Flows on Particle Tracking. U.S. Department of Interior Bureau of Reclamation.

U.S. Fish and Wildlife Service. 2008. Formal Endangered Species Act Consultation on the Proposed Long-Term Operations of the Central Valley Project and State Water Project. Memorandum from Regional Director, Fish and Wildlife Service, Region 8, Sacramento, California, transmitting the Biological Opinion to Operation Manager, Bureau of Reclamation, Central Valley Operations Office Sacramento, California. December 15, 2008.

U.S. Fish and Wildlife Service. 2024 Biological Opinion: Reinitiation of Consultation on the Coordinated Long-Term Operation of the Central Valley Project and State Water Project. U.S. Fish and Wildlife Service. November 8, 2024. Available at: https://cawaterlibrary.net/document/2024-biological-opinion-reinitiation-of-consultation-on-the-coordinated-long-term-operation-of-the-central-valley-project-and-state-water-project/

Wang, X., P. Russell, A. Pope, D. Jackson, and D. Hance. 2024. Individual-Based Ecological Particle Tracking Model (ECO-PTM) for Simulating Juvenile Chinook Salmon Migration and Survival Through the Sacramento–San Joaquin Delta. San Francisco Estuary and Watershed Science, 22(4). https://doi.org/10.15447/sfews.2024v22iss4art4

Windell, S., P.L. Brandes, J.L. Conrad, J.W. Ferguson, P.A.L. Goertler, B.N. Harvey, J. Heublein, J.A. Israel, D.W. Kratville, J.E. Kirsch, R.W. Perry, J. Pisciotto, W.R. Poytress, K. Reece, B.G. Swart, and R.C. Johnson. 2017. Scientific framework for assessing factors influencing endangered Sacramento River winter-run Chinook salmon across the life cycle (NOAA Technical Memorandum NMFS-SWFSC-586). U.S. Department of Commerce. https://doi.org/10.7289/V5/TM-SWFSC-586

Zeug, S.C., and B.J. Cavallo. 2014. Controls on the Entrainment of Juvenile Chinook Salmon (Oncorhynchus tshawytscha) into Large Water Diversions and Estimates of Population-Level Loss. PLoS ONE, 9(7), e101479. https://doi.org/10.1371/journal.pone.0101479

Zhang, Y.J., N. Gerdts, E. Ateljevich, and K. Nam. 2020. Simulating vegetation effects on flows in 3D using an unstructured grid model: Model development and validation. Ocean Dynamics, 70(2), 213–230. https://doi.org/10.1007/s10236-019-01333-8